Role of Mitochondrial dynamics and activity in epithelial cell remodelling during *Drosophila* oogenesis

A Thesis
submitted to
Indian Institute of Science Education and Research Pune in partial fulfilment of the requirements for the BS-MS Dual Degree Programme
by
Mridusmita Das

Indian Institute of Science Education and Research Pune
Dr. Homi Bhabha Road, Pashan, Pune 411008, INDIA.
Date: April, 2024
Under the guidance of
Supervisor: Prof. Richa Rikhy, Co supervisor: Prof. Muriel Grammont
Department of Biology
From May 2024 to Mar 2025
INDIAN INSTITUTE OF SCIENCE EDUCATION AND RESEARCH PUNE

Certificate

This is to certify that this dissertation entitled Elucidation of the **Role of Mitochondrial dynamics and activity in epithelial cell remodelling during *Drosophila* oogenesis** towards the partial fulfilment of the BS-MS dual degree programme at the Indian Institute of Science Education and Research, Pune represents study/work carried out by Mridusmita Das at Indian Institute of Science Education and Research and LBMC, ENS Lyon under the collaborative supervision of Prof. Richa Rikhy, Chair Biology, Department of Biology and Prof. Muriel Grammont, Principle Investigator, LBMC ENS Lyon during the academic year 2024-2025

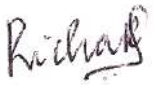

Prof. Richa Rikhy

Prof. Muriel Grammont

Committee:

Prof. Richa Rikhy

Prof. Muriel Grammont

Prof. Girish Ratnaparkhi

This thesis is dedicated to my parents and my sister.

Declaration

I hereby declare that the matter embodied in the report entitled “Role of Mitochondrial dynamics and activity in epithelial cell remodelling during *Drosophila* oogenesis” are the results of the work carried out by me at the Department of Biology, Indian Institute of Science Education & Research (IISER) Pune and Ecole normale supérieure de Lyon, France under the supervision of Prof. Richa Rikhy and Prof. Muriel Grammont respectively and the same has not been submitted elsewhere for any other degree. Wherever others contribute, every effort is made to indicate this clearly, with due reference to the literature and acknowledgement of collaborative research and discussions.

Mridusmita Das
20201247

Table of contents

List of Tables and Figures

List of Tables:

List of Figures:

Chapter 1

Chapter 2

Chapter 3

Abstract

Mitochondria are famously known as the powerhouse of the cell and play an important role in regulating the production of ATP, reactive oxygen species, metabolites and buffering calcium for various activities in a eukaryotic cell. Epithelial cell differentiation accompanies the formation of elaborate and active mitochondria. Mitochondrial dynamics involves fusion and fission and occurs with the help of the Dynamin family of GTPases. Here we aimed to study the role of mitochondrial dynamics and activity in regulating follicle epithelial cell shape remodelling in *Drosophila* oogenesis. Follicle cells are known to change shape from cuboidal to squamous due to increase in cytoplasmic pressure generated in the form of a gradient by the underlying germ cells. In contrast, the cells in the central and posterior region transit from cuboidal to columnar. We found that when mitochondrial fusion and fission is depleted in follicle cells, there is an alteration in cell shape remodelling in follicle cells. Future studies will allow us to understand the mechanisms by which this epithelial cell remodelling is affected in follicle cells.

Acknowledgements

It is genuine pleasure to express my deep sense of thanks and gratitude to my supervisor Prof. Richa Rikhy, Chair Biology, Department of Biology and Prof. Muriel Grammont, Principal investigator at Department of LBMC (Laboratoire de biologie et de modélisation cellulaire), ENS Lyon for her guidance and support. I would also like to thank all the lab members for their advice and help. Finally, I would like to thank IISER Pune and Ecole Normale Superieure de Lyon for providing me with the infrastructure to carry out my work. Additionally I would like to thank the *Drosophila* and IISER Pune Microscopy facility as well as the Platim facility at ENS Lyon without whom it would not have been possible .

Contributions:

Contributor name	**Contributor role**
Mridusmita Das, Richa Rikhy, Muriel Grammont	Conceptualization Ideas
Richa Rikhy, Muriel Grammont	Methodology
—	Software
Mridusmita Das	Validation
Mridusmita Das	Formal analysis
Mridusmita Das	Investigation
Richa Rikhy, Muriel Grammont	Resources
Mridusmita Das	Data Curation
Mridusmita Das	Validation
Mridusmita Das	Writing - original draft preparation
Mridusmita Das, Richa Rikhy	Writing- Review and editing
Mridusmita Das	Visualization
Richa Rikhy, Muriel Grammont	Supervision
Mridusmita Das	Project administration
Richa Rikhy, Muriel Grammont	Funding acquisition

Chapter 1

INTRODUCTION

1.1. Epithelial tissues and epithelial cell shape remodelling

Cells change shape to facilitate different morphological processes. Morphogenesis is the fundamental phenomenon during organ formation. Epithelial tissue lining their outer and inner surface determines the structure of the organs. These epithelial tissues undergo several remodelling processes during development, such as invagination and tissue elongation to structure organs properly (Ettensohn, 1985; Sutherland et al., 2020). This defines epithelial morphogenesis. Two examples of epithelial morphogenesis; invagination and tissue elongation like cell shape change during development and are considered one of the most critical processes in epithelial morphogenesis. Cell shaping must be tightly regulated as any defects in the change of cell shape will lead to severe problems, such as tissue elongation. It is one of the most common morphogenetic processes observed at different stages of development of palate and lip. Several common dysmorphologies that occur due to tissue elongation failure, such as cleft palate formation (Parker et al., 2010), exemplify its importance in development.

1.2. Morphogenesis - the fundamental process of cell shape change in tissue formation

The structures of organs are determined by the epithelial tissue lining their outer and inner surface. Here I present two examples of epithelial morphogenesis; invagination and tissue elongation.

1.2.1. Invagination as a morphogenetic process

Epithelial invagination is the morphological process in which three-dimensional epithelial pit or furrow structures are formed from flat sheets of epithelial tissue. The cells initially undergo apical constriction during this process that leads to a reduction of apical surface and cell elongation along the apical-basal axis. These processes cause the cell to change shape from cylindrical to wedge-shaped. This is followed by basal expansion and cell shortening, causing the formation of deep pits (Chauhan et al., 2015; Kondo and Hayashi, 2015). Invagination is essential during the development of pit or cup-like structures such as the inner ear and nasal cavity (Hilfer et al., 1989; Shindo, 2018) and in processes such as gastrulation and neurulation, which involves furrow formation.

1.2.2. Tissue elongation as a morphogenetic process

The cellular process of tissue elongation, which ultimately demands increases in the number or size of the cells along the axis of elongation, can be divided into four types (Fig.1.2.1) (Economou et al., 2013). Most simply, tissue elongation can occur by localized cell proliferation, leading to increased cell number. This method of tissue elongation is observed in vertebrate long bone formation and plant meristems. Similarly, cell divisions along the axis of growth due to anisotropy in cell division's orientation also contribute to tissue elongation (Gong et al., 2004; Lechler and Fuchs, 2005). Other than cell division, cell number increase along the direction of elongation by cell movements and rearrangements as in convergent

extension where cells intercalate with the help of actin-rich protrusions (Keller, 2006) or junction remodelling, followed by neighbour exchange also leads to tissue elongation (Irvine and Wieschaus, 1994). Finally, elongation of tissue also occurs by elongation of component cells along the direction of tissue elongation as observed in growing plant roots and elongation of *Drosophila* follicle (Baluska et al., 1996). However, the tissue elongation process observed during development involves a combination of these mechanisms, with each contributing to a different extent. (Figure 1.2.1) For example, cell shape change and cell Intercalations are required for *Drosophila* germ band extension (Blanchard et al., 2009) .

This study concentrates on the epithelial cell shape changes that lead to tissue elongation.

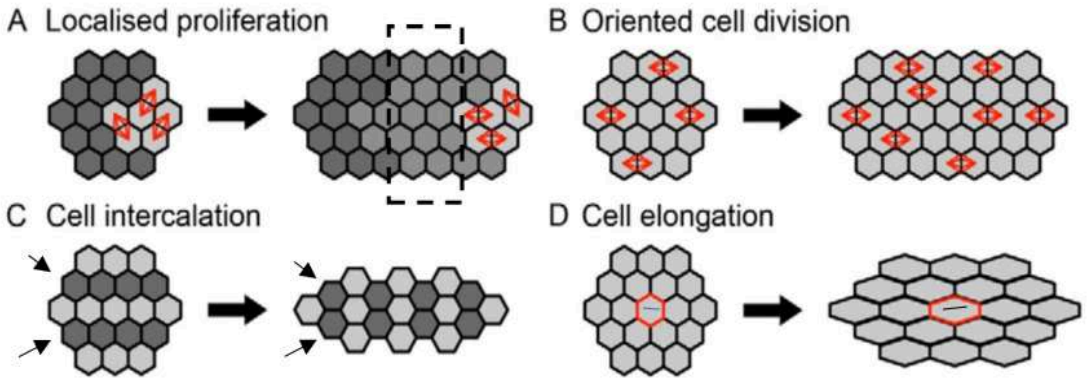

Figure 1.2.1. Schematic representation of the four methods by which tissue elongates.

A) cell divisions localized to one edge of the tissue lead to cell elongation towards that edge. (B) Cell division and alignment of daughter cells along one direction leads to tissue elongation. (C) Tissue elongation by cell intercalation includes the movement of cells perpendicular to the direction of growth with the help of actin protrusion or neighbour exchange (D). Tissue elongation as result of cell elongation. (Image modified from Economou et al., 2013).

Epithelial tissues are one of the four different tissues present in animals. This section explains the classification of epithelia and their two major characteristics. Epithelial cells can be classified based on their number of layers and their shape.

Classification based on layers of cells: Epithelia can be classified as simple, stratified, and pseudostratified based on the number of layers they comprise. Here simple epithelia are composed of a single layer of cells, stratified epithelia cells are composed of more than one layer of cells, and pseudostratified epithelia are composed of only one layer of cells but appear to have several layers due to differences in the size of cells.

Classification based on the shapes of cells: Three types of epithelial cells, classified based on their shapes, are observed in animals. They include squamous, cuboidal, and columnar epithelial cells. The division is based on the proportion of height and width of the cells. While squamous epithelial cells have more width than height, the cuboidal epithelial cells have equal width and height. Unlike the other two, columnar cells have more height than the width. They maintain the cell shape or undergo a transition from one cell shape to another

as required to structure organs and carry out their functions effectively. (Figure 1.2.2)

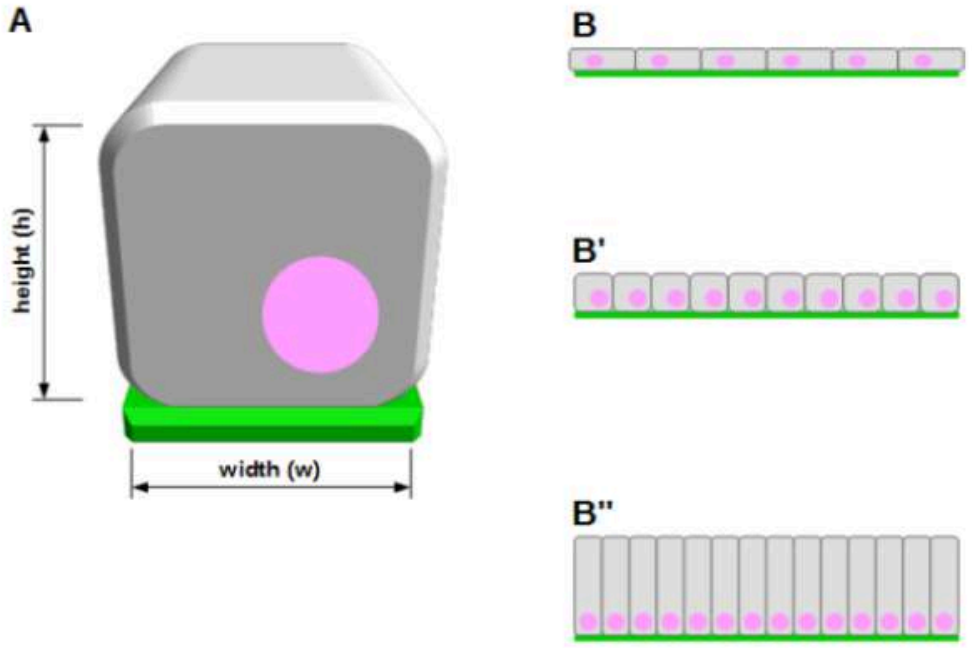

Figure 1.2.2 Classification of squamous, cuboidal and columnar cells. In all panels, the basement membrane is coloured in green, the epithelial cells in light grey, and their nuclei in pink. The basal domain of the cells faces towards the basement membrane. (A) The ratio of cells height and width is used to classify cells into (B) squamous, (B') cuboidal, and (B'') columnar (Image adapted from Lamiré et al., 2019)

1.3 Epithelial cells, polarity and shape regulation

Epithelial cells are characterized by their adherent and polarized nature. These characteristics are essential for them to carry out their functions.

Polarised nature of epithelial tissues

The spatial arrangement of several protein complexes polarizes the epithelia into various domains as apical, basal, and lateral, with each domain involved in different functions (Wang and Margolis, 2007). The Crumbs complex composed of Crumbs, Stardust, Disklost, and Par complex Bazooka, α PKC, Par6, Cdc42 are the major proteins localized in the apical domain. They play a role in defining the apical polarity and excluding basolateral determinants from the apical domain (Tepass et al., 1990; Wodarz et al., 1995). The major proteins in the lateral domain include Lethal Giant Larvae, Disc Large, and Scribble complex (in mature epithelia). They maintain the lateral identity by excluding the apical proteins from the lateral domain (Bilder and Perrimon, 2000). The basal domain establishes its identity by interacting with the basement membrane with the help of focal adhesion complexes, of which integrin is a vital component. Interaction with the basement membrane, specifically laminin, is required for the proper spatial arrangement of apical proteins and overall cellular polarisation (Klein et al., 1988; Rasmussen et al., 2012)

Adhesive property of epithelial tissue

The epithelial cells adhere to each other and the basement membrane with the help of several junctions.

Cell-Basement Membrane Adhesion

The adhesion between the cell and the basement membrane is facilitated by focal contacts composed of integrins that link Actomyosin via Talins to BM. In addition to adhesion, they also act as mechanosensors (Riveline et al., 2001).

Cell-Cell Adhesion

In invertebrates, the cells adhere to each other with the help of adherens junction, septate junctions, and gap junctions present on the lateral domain. However, in vertebrates, the tight junction instead of the septate junction, along with the adherens junction and gap junction, facilitate cell-cell adhesion. Among these junctions, adherens junctions importance in governing the cell's shape is clearly established (Aguilar-Aragon et al., 2020; Pinheiro and Bellaïche., 2018). Since our study explores the role of cell-cell junction contributed by adherens junction in cell shaping, its characteristics will be explained in detail.

Epithelial cell shape changes are regulated by:

Cell-cell contacts

The geometry of a cell largely depends on its interaction with its neighbouring cells. Hence maintenance and remodelling of the cell-cell junction are significant factors determining the cell's shape (Priess and Hirsh, 1986). Several studies prove that the cell-cell contacts between epithelial cells maintained via the adherence junction play a vital role in dictating their shape (Carthew, 2005). The importance of adherens junction remodelling In bringing about cell shape changes is observed during intercalation (Kane et al., 2005). Changes in the cell's shape that facilitate intercalation involve disassembly followed by the assembly of the new adhesive junction in radial intercalation event or reordering of adhesion junction in planar intercalation. Hence, any disruption in AJ's disassembly, assembly, and reordering process would affect cell shape changes and thereby the intercalation. Moreover, the importance of E-cadherin maintenance and remodelling in cell shaping was confirmed by studies where the perturbation of factors that regulate E cad’s localization causes defects in cell shape. Hence, we can conclude from these studies that dynamicity and level of Ecad in adherens junction are vital for proper cell shape changes.

Cytoplasmic pressure

The role of cytoplasmic pressure in regulating the cell shape is not adequately understood. Some studies have shown that cytoplasmic pressure is essential for rounding of cells during mitosis (Stewart et al., 2011) and embryo size control (C. J. Chan et al., 2018). Cell shape changes require the involvement of mainly cell-cell adhesion and cell contractility. Before elongation, the Actin bundles attached to the AJ are present perpendicular to the anterior-posterior axis. During elongation, they undergo shortening and thickening. When

the adherence junction is distorted by a mutant Ecad, the Actomyosin detaches from the AJ and prevents cell elongation. In this case, the Actomyosin shortening is not affected (Costa et al., 1998).

Due to adhesion to the basement membrane:

Epithelial cells are characterized by their adherent and polarized nature. These characteristics are essential for them to carry out their functions like barrier function, mechanical support, and selective transportation. The spatial arrangement of several protein complexes polarizes the epithelia into various domains as apical, basal, and lateral, with each domain involved in different functions (Wang and Margolis, 2007). *Drosophila* follicular epithelium surrounding germ cells and resting on a basement membrane is an excellent system to study the regulation of the epithelial cell shape changes.

1.4. The *Drosophila* ovarian follicle as a model to study the epithelial morphogenesis

Drosophila follicular epithelium surrounds nurse cells and rests on the basement membrane. It is an excellent system to study the regulation of the epithelial cell shape changes. Its well-defined structure helps identify the extrinsic forces acting on it, and its well-characterized developmental pattern helps identify intrinsic factors acting on the cells. Easy access and availability of many follicles in each ovary is another practical advantage of this model.

Structure of the ovaries: Female *Drosophila* have a pair of ovaries composed of 16 to 20 ovarioles. Each ovariole contains a germarium where the ovarian follicles are formed and the vitellarium that houses several developing ovarian follicles in different stages of their maturation (Figure 1.4.1). The complete maturation of follicles takes place through 14 different stages (King et al., 1970), starting with the formation of the follicle at stage 1 and ending with the emergence of a fully formed egg at stage 14. A follicle comprises 16 germline cells, including one oocyte located posteriorly and 15 nurse cells located anteriorly, surrounded by a monolayer of somatic epithelium that rests on an outer basement

membrane. (Figure 1.4.1)

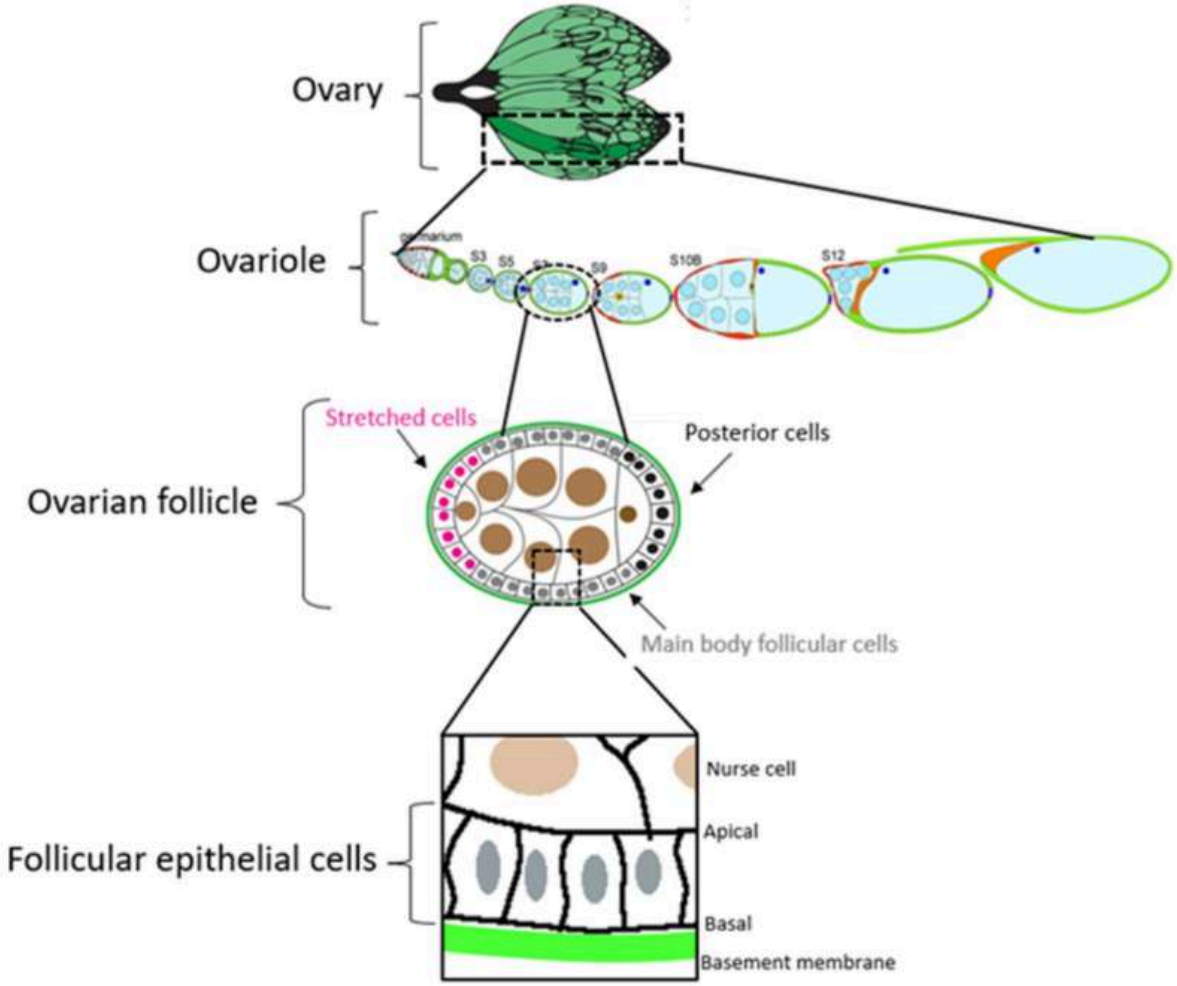

Figure 1.4.1. Female *Drosophila* have a pair of ovaries composed of 16 to 20 ovarioles in each ovary. The ovariole consists of a germarium and developing ovarian follicles. Each follicle comprises a cyst surrounded by differentiated cells. The apical domain of the epithelial cells faces the nurse cells. In the figure, the anterior is to the left (adapted from google images).

Formation of epithelial ovarian follicle

The germarium in which the follicles are formed is divided into three different regions. Follicle formation starts at region 1, which houses 2 or 5 germline stem cells that give rise to a cytoblast that undergoes four rounds of symmetric and synchronous divisions to develop into a cyst of 16 cells. These cells share a circular cleavage furrow called ring canals due to incomplete cytokinesis. The number of ring canals (RC) each cell bears ranges from 1 to 4 and depends on the pattern of their formation. Of the 16 germline cells, one of the two cells with 4 RC develops into the oocyte. Once the formed cyst enters regions 2, 2-14 somatic stem cells present in this region give rise to 16 somatic epithelial cells that surround the cyst. When the follicle enters region 3, which is also stage 1 of its maturation, the cyst would be entirely covered by around 100 follicular epithelial cells. This whole process of follicle formation in the germarium takes around seven days. Following this, the fully formed ovarian

follicle exits the germarium to enter the vitellarium as a round structure composed of germline cells of similar volume, surrounded by around 200 epithelial FC resting on a BM (Figure 1.4.2)

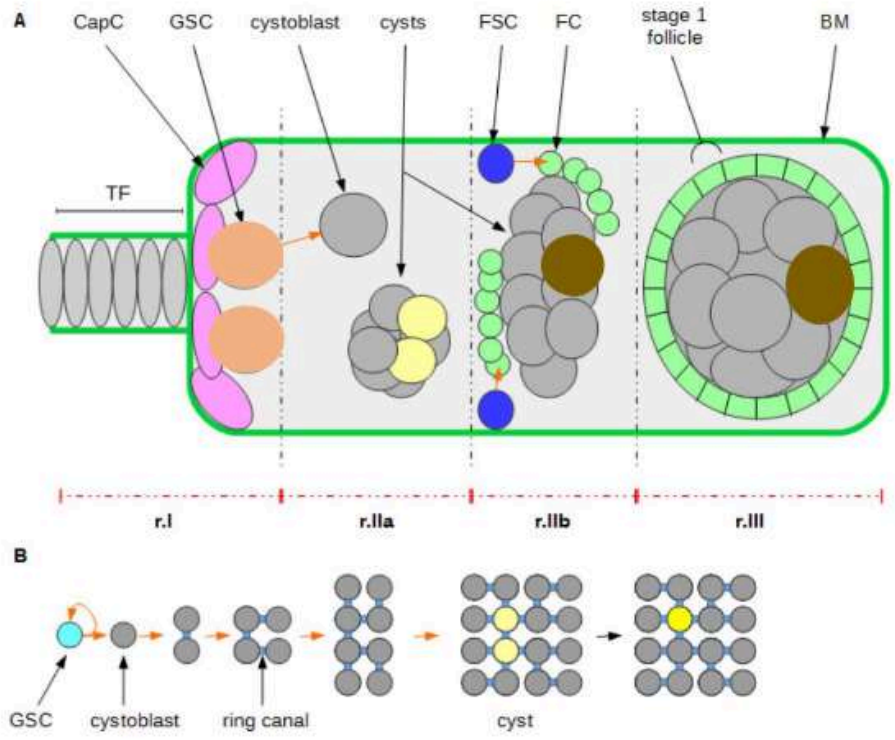

Figure 1.4.2 : The germarium covered by a basement membrane is composed of 4 regions, each playing a role in follicle development. Region 1, present on the anterior-most part, comprises terminal filaments, cap cells, and germinal stem cells. In region IIa, the cytoblast formed from GSC develops into a cyst. Later in region 2b, selection of one of the cyst cells to form the oocyte and division of SFC to generate FC that surround the cyst takes place. (B) The 16 celled cyst formation starts from GSC by 4 synchronous, but incomplete cell division to create connections called ring canals. The number of ring canal's each cell possess depends on the cell division pattern, resulting in two cells to have 4 ring canals, two cells to have 3 ring canals, four cells to have 2 ring canals, and eight cells to have 1 ring canal (Image adopted from Lamiré et al., 2019).

Maturation of epithelial ovarian follicle

From stage 1 to stage 14 in the vitellarium, the different follicle components undergo several changes necessary for the development of a mature egg in 3 days. Changes observed in Basement membrane during follicle maturation: The extracellular matrix or basement membrane composed of Collagen IV, Laminin, Nidogen, and Perlecan (Yurchenco, 2011) is a critical component that assists follicle elongation. The components that constitute the BM are mainly secreted by the follicular cells. Their rotation around the static BM in the anterior-posterior direction from stages 2 to 8 (Horne-Badovinac, 2014) allows the deposition of these components in fibril-like structures aligned perpendicular to the anterior-posterior axis in addition to bulk deposition (Isabella & Horne-Badovinac, 2016). Studies have shown that the BM is necessary for the proper follicle elongation as it acts as an external constraint, allowing only anterior-posterior growth of the follicle (Chlasta et al., 2017). Moreover, its differential stiffness, with its edges being softer compared to the centre,

also helps to accommodate the expansion of cells during follicle elongation (Crest et al., 2017).

Changes in Germline cells (nurse cell (NC) and oocyte) during follicle maturation

The NCs are metabolically highly active cells that synthesize and transfer various proteins and mRNA to the oocyte, which are necessary for its growth and the development of the future embryo through their ring canals. The growth of the NC during egg formation can be classified into two broad phases. Their growth rate remains constant from stage 1 to stage 8, and they undergo endoreplication except for the oocyte, whose replication is arrested in prophase 1 of meiosis (Hyun et al., 2009). During these stages, the follicle remains round in shape.The NC undergoes enormous growth from stages 8 to 10, and the follicle undergoes elongation. Throughout these stages, the transfer of components to the oocyte continues but in a non-specific manner, such that by the end of stage 10, the volume of the oocyte becomes similar to the volume of all the NC summed up together. Following their last transfer at stage 11, they undergo degeneration (Timmons et al., 2016; Kolahi et al., 2009)

Changes Follicular epithelial cells undergo during follicle maturation

During the different stages of maturation, the FC undergo proliferation, differentiation and cell shape changes. Stage 1 to 6 is their phase of proliferation, where FC undergoes six divisions to give rise to around 850 cells to accommodate the initial growth of the NC. After stage 6, they stop dividing but undergo three rounds of endoreplication. The formed FCs undergo differentiation and adopt different fates such as polar cells, border cells, centripetal cells, columnar cells, and stretched cells (Figure 1.4.3)

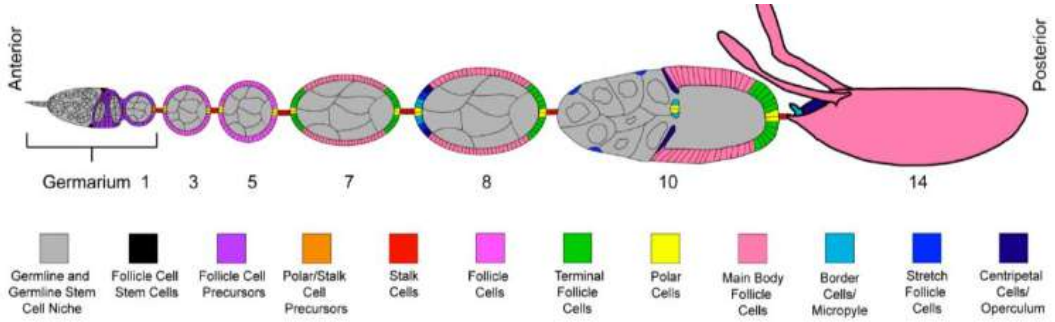

Figure 1.4.3 The maturation of the follicle takes place in 14 stages. The maturation involves the growth of the NC in two phases, from stage 1 to 8 and stage 9 to 11. As a result, the follicle grows from stages 1-8 but remains round but grows and elongates during stages 9-11. Also, the FC, which undergoes division to accommodate the initial NC growth, differentiates into different cell types, two of which undergo cell shape changes to accommodate the second phase of NC growth (Image adopted from Lamiré et al., 2019).

The polar cells – They include two pairs of cells present on the anterior and posterior pole of the follicle whose differentiation is controlled by Notch signalling (Grammont and Irvine, 2001). They are crucial in deciding the nearby cell's fate as border cells, stretched cells, centripetal cells, and posterior cells

Border cells – They are composed of 6-8 cells present at the anterior pole adjacent to polar cells. At stage 9, they, together with polar cells, migrate to join the oocyte.

The centripetal cells – They include the cells present at the NC-oocyte junction at the border between columnar cells and StC. They undergo radial migration to line the anterior region of the oocyte.

Columnar cells – They include cuboidal cells present on the posterior region of the follicle that undergo cuboidal-columnar cell shape transition at stage 9 (S9) to give rise to around 800 columnar cells covering the growing oocyte (Fig. 7). Studies show that the columnar cells play a vital role in establishing the axis of the oocyte and deposit the vitelline membrane and chorion of the future egg (Lilly and Spradling, 1996; Maines et al., 2004). This cuboidal-columnar transition is one of the cell shapes changes this study explores.

Stretched cells (St C) – StC includes around 50 cuboidal cells present in the anterior region of the follicle that undergoes cuboidal-squamous cell shape transition at S9 to accommodate the massive growth of the nurse cell. During this transition, the StC reduces height and expands the apical and basal region (Fig.7). This transition, which occurs like a wave in the anterior to posterior direction, requires remodelling of adhesive junctions (Grammont, 2007). This cuboidal- squamous transition is the cell shape change I am interested in exploring.

1.5 Cell shape changes in *Drosophila* follicle cells

Formation of epithelial ovarian follicle: The germarium in which the follicles are formed is divided into three different regions. Follicle formation starts at region 1, which houses 2 or 5 germline stem cells that give rise to a cystoblast that undergoes four rounds of symmetric and concurrent divisions to develop into a cyst of 16 cells. These cells share a circular cleavage furrow known as ring canals which occurs because of incomplete cytokinesis. The follicle cells transits cuboidal to columnar and cuboidal to squamous cell shape transitions in stage 9 oogenesis (Figure 1.3.1).

Epithelial cells which are the main component of our tissues and organs and can be of 3 forms (cuboid, columnar and squamous) are attached to each other, also they are attached to a basement membrane. Epithelial cells often change shape and this depends on cell adhesion and cell contractility. The later is regulated by energy production, which depends on mitochondrial organisation and activity. The germ cells underneath are covered by follicle cells which form as a covering or epithelium. The egg shell is given rise by several morphological changes as the follicle cells under various cell shapes change during the duration of oogenesis.

Three ovarian follicles are represented at three different stages from early to late. At an early stage, the epithelial cells (pink, grey and black) are cuboid. They surround the Germ cell (brown) and rest on a basement membrane (green) (Figure 1.5.1)

At the middle stage, a gradient of cytoplasmic pressure is generated in inner nurse cells(red arrows) exerting strong pressure on the anterior cells (left side). Stiffness of Basement membrane also presents a gradient. The mechanical properties combined compresses more the anterior epithelial cells (pink) than central or posterior (grey/ black). Thus the pink cells become squamous while others are columnar.

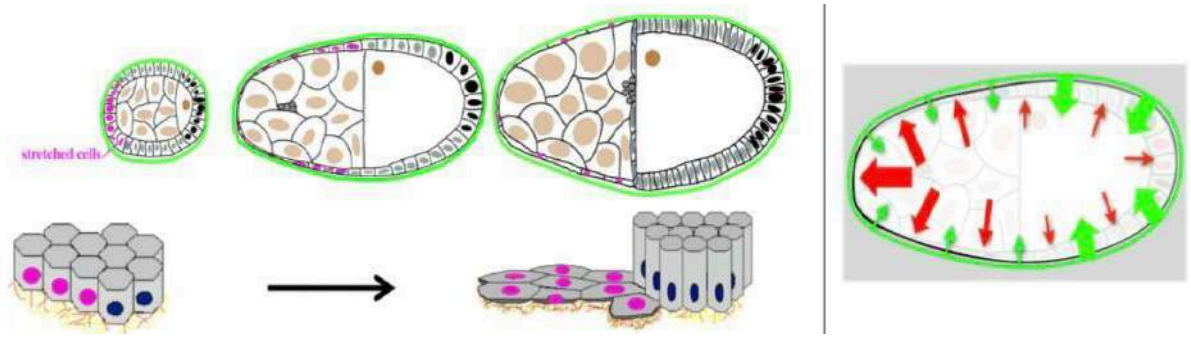

Figure 1.5.1. A) Schematic representation of the growth and elongation of the ovarian follicle. B) Schematic representation of the cuboidal-to-squamous and cuboidal-to-columnar transitions the follicular epithelial cells undergo during stage 9 of oogenesis (Image adapted from Brigaud et al., 2015)

Adherens junction remodelling during the cuboidal - columnar- squamous transition

Adherens junction remodelling during the cuboidal-squamous transition: The adherens junctions undergo a progressive remodelling starting from the anterior-most stretched cells and progressing to posterior stretched cells. It starts with the remodelling of adherens junctions on the anterior three-cell vertices, followed by the adherens junctions on the anterior membrane perpendicular to the A/P axis and the adherens junction on the posterior three-cell vertices allowing expansion of the apical domain along the anterior-posterior axis. (Figure 1.5.2) This process is continued row by row to give rise to flat, anisotropic cells covering the NC (Grammont, 2007).

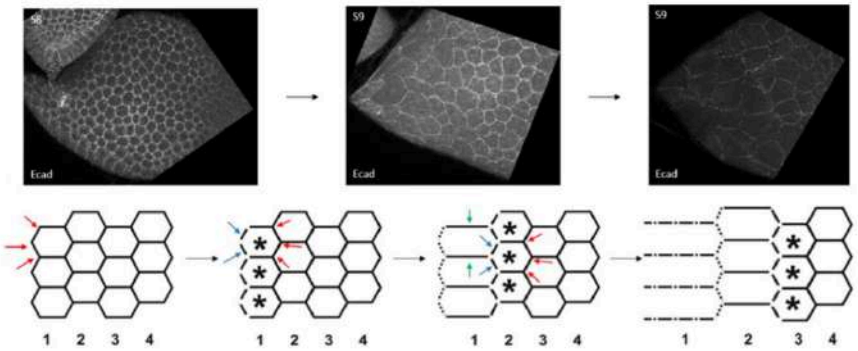

Figure 1.5.2. Progressive remodelling of adherens junction observed during StC flattening. Schematic representation of the model of adherens junction remodelling (Schematic representation adopted from Grammont, 2007)

Factors regulating cell elongation and flattening:

Genes such as hindsight and signalling pathways such as the Notch pathway and TGF-β pathway have been shown to regulate cell shaping by controlling the AJ remodelling (Chlasta et al., 2017; Grammont, 2007; Melani et al., 2008). The gene hindsight encoding Hindsight TF regulates StC flattening by controlling the accumulation of the adhesion proteins such as

Ecad, Ncad, and β- Catenin. The mutant cells for this gene exhibit defective flattening and reduced apical and basal surface area (Melani et al., 2008).

Germline pressure

Recent data have shown that the growing germline cells exert a force on the overlying StC and the flattening of StC depends on the tension it experiences due to this force (Figure 1.5.3) (Balaji et al., 2019). In wild-type, it is observed that a pressure difference exists between adjacent NCs as the NC membrane in 2-dimensional pictures of stage 9 or 10 follicles appear convex to the posterior pole. However, the membrane of the NC just adjacent to the oocyte remains straight, indicating the absence of such a pressure difference between NC and the oocyte. This curvature is more prominent on the anterior part than the posterior part indicating that the pressure difference is more pronounced in the anterior part. These observations were confirmed by AFM measurements (Figure 1.5.3)

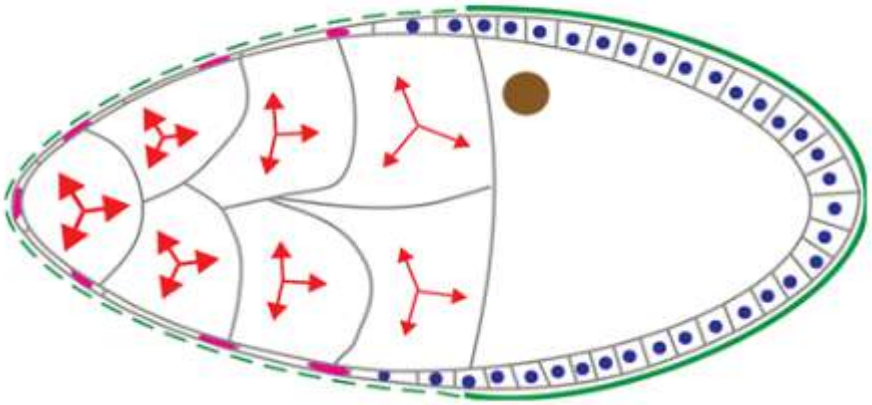

Figure 1.5.3 Schematic representation of the force exerted by the nurse cells on the epithelial cells presented above. Basement membrane(green), oocyte (brown coloured nucleus), Stretched cells (StC) (pink), Main body follicular cells (blue). The red arrows depict the pressure within the nurse cells, and the width of the arrows indicates the magnitude of the pressure (Adopted from Lamiré et al., 2020)

Basement membrane and StC flattening.

The importance of the interaction of StC with BM for its flattening has been well established. Studies demonstrate that follicles mutant for Integrin subunit show defective flattening of StC (Huang et al., 2021). Supporting this, early or delayed expression of the gradient of basement membranes' stiffness leads to delayed or premature flattening of StC (Chlasta et al., 2017).

Mitochondrial fission fusion protein was identified to regulate the transition of epithelial cells from cuboidal to squamous. However, its function remains unclear.

1.6. Mitochondria and their function in cell shape remodelling

Mitochondrial dynamics: Mitochondria are famously known as the powerhouse of the cell and play an important role in regulating the production of ATP, reactive oxygen species, buffering Calcium for various activities in a eukaryotic cell. Mitochondrial fission is a process which occurs when a single mitochondrion divides into two daughter mitochondria, which is driven by the Dynamin related protein (Drp1) at the actin and Endoplasmic Reticulum (ER) mediated constriction sites. Mitochondrial fusion process where the outer membrane fusion is driven by Mitofusins 1 and 2 (*Drosophila* Marf), and the inner membrane with the help of Optic atropy1 (Opa1). The cellular needs of the cell are maintained by these fusion fission transitions and also they ensure that the mitochondria keeps functioning well. (Figure 1.6.1).

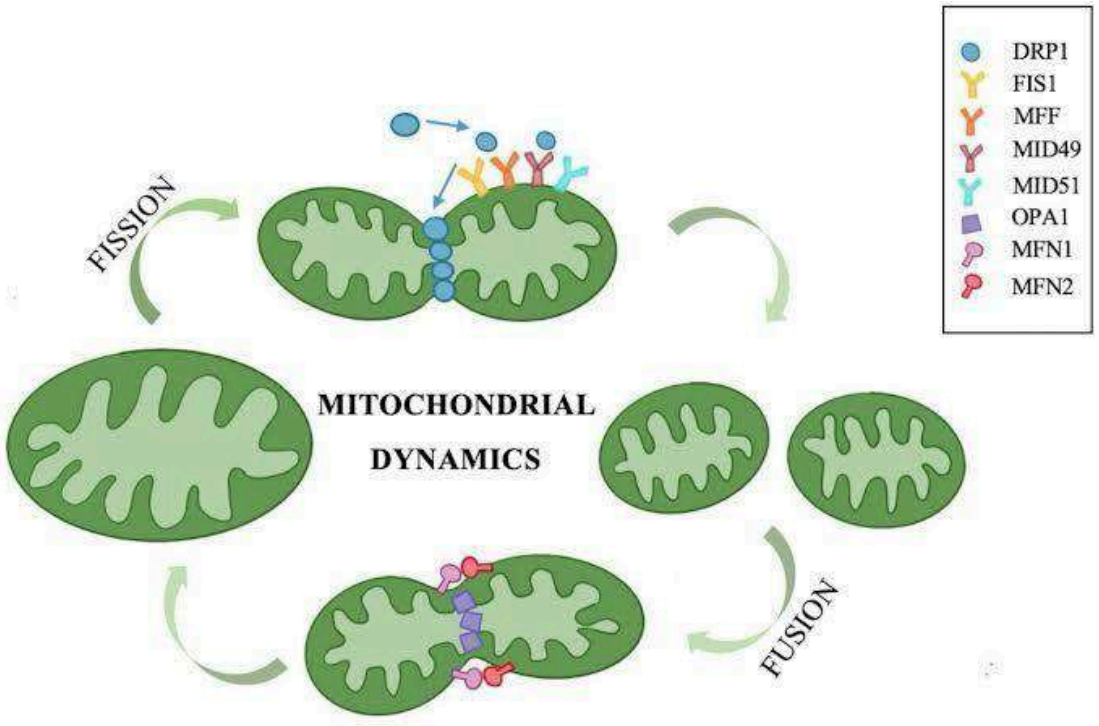

Figure 1.6.1 . Schematic representation of mitochondrial dynamics (adapted from Xiang et.al, 2022)This illustration depicts the dynamic behavior of mitochondria, including key processes such as fission, fusion. Mitochondrial fusion facilitates the mixing of mitochondrial contents and supports metabolic efficiency, while fission contributes to mitochondrial distribution, quality control, and apoptosis.

Mitochondrial role in formation of epithelial cells: Transition of mitochondria from spherical to elongated shape during epithelial cell formation (Figure 1.6.2). An increase is seen in the ATP generating ability (light green gradient) by mitochondria which elongate during the process of epithelial cell remodelling (B-E). Epithelial to mesenchymal transition (EMT) occurs due to loss of polarity proteins. Previous studies from our lab demonstrate how mitochondria dynamically regulates distribution of polarity proteins. From fig G to I, there is a change in mitochondrial shape from elongated to spherical like structure. Here epithelial polarity is lost on EMT during several processes. The migratory ability to the cell is brought by EMT. They do it by detaching and losing polarity complexes (I). F to I, there is a decrease in ATP generating ability during EMT where the mitochondria is fragmented. Decrease in Ros levels is seen during formation of epithelial cells and increases during transiting from Epithelial to mesenchymal cells. (Figure 1.6.2)

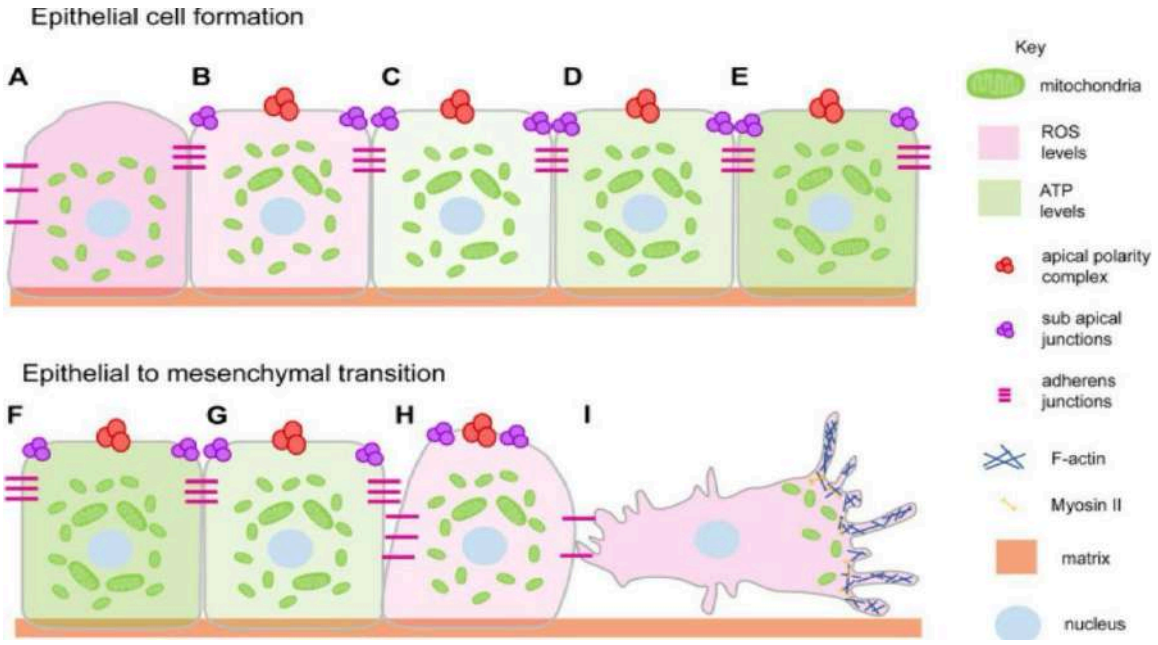

Figure 1.6.2. Schematic representation of mitochondrial dynamics in regulating epithelial cell remodelling (Madan et. al, 2022)

1.7 Aims of the project

The main aim of my project is to decipher the role of mitochondria distribution and dynamics in regulating epithelial cell remodelling. To address this aim better we are studying the role of mitochondrial dynamics and activity in regulating follicle epithelial cell shape remodelling in *Drosophila* oogenesis. Follicle cells are known to change shape from cuboidal to squamous due to increase in cytoplasmic pressure generated in the form of a gradient by the underlying germ cells. In this project we will test the change in mitochondrial distribution and activity during the cuboidal to squamous cell shape transition. We will use genetics to perturb mitochondrial dynamics and activity to elucidate the role of mitochondrial activity in follicle cells and/or the underlying germ cells in supporting the follicle cell shape change. We will use a dominant negative mutant for Drp1 to deplete the mitochondrial fission activity and use RNAi to deplete mitochondrial fusion protein Marf. This project hopes to reveal the mechanism by which mitochondrial activity and metabolism regulate key interactions between the germ line and follicle cells for morphogenetic events in development.

Chapter 2

MATERIALS AND METHODS

2.1. *Drosophila* stocks and crosses

The Drosophila lines used in this study are indicated in table 1.

Table 1.

No:	Genotype	Sources
1	w^{1118}	Bloomington *Drosophila* Stock Centre
2.	$DRP1^{SG}$	Rikhy Lab
3.	Marf1 RNAi	Ming Guo lab
4.	ND-51 Complex 1 Subunit RNAi	Bloomington *Drosophila* Stock Centre
5.	GR- Gal4	Girish Ratnaparkhi's lab
6.	UAS Mito-GFP	Sayali Chowdhury, Rikhy Lab
7.	*nanos*-Gal4, Mito-GFP	Sayali Chowdhury, Rikhy Lab
8.	*hs-Flp*;Act-FRTstopFRTGal4, UAS-GFP/CyO	Grammont lab

Fly crosses were incubated at 25 degree Celsius. Each cross used ten virgin female flies from the Gal4 line and five males from the UAS line per vial. Two replicates of each cross were performed simultaneously, and the parents were transferred into fresh media vials every three days.

2.2 Generation of *Drosophila* lines of required genotype

Drosophila melanogaster possesses four chromosomes that include the X and Y sex chromosome (also referred to as chromosome 1), two large autosomes (referred to as 2nd and third chromosome), and a fourth dot chromosome (Metz et al., 1914). These chromosomes undergo meiotic recombination in germline cells of female *Drosophila*. However, this is not observed in males. This phenomenon has several advantages in many genetic studies, but this makes it unable to track and maintain mutations during *Drosophila* stock establishment. Hence, to overcome this, We use balancer chromosomes. Balancer chromosomes are multiply inverted rearranged chromosomes that prevent the recovery of mitotically recombined chromosomes and suppress meiotic recombination. Recessive lethal or sterile mutations and dominant visible markers they carry prevent them from being homozygous and help track their inheritance in crosses, respectively. In addition to their use in *Drosophila* stock generation, they also help maintain deleterious or sterile alleles in stocks (Miller et al., 2018).

2.3. The establishment of *Drosophila* lines includes several steps:

2.3.1. Sorting

● Male and female flies

The sexing of flies was performed based on the characteristics of their genitalia at the tip of their abdomen. While males possess dark and rounded genitalia, females have light and pointed genitalia. In addition, a small patch of bristles called sex combs present on the foreleg of males but absent in females also help in sexing flies.

● Virgin and mated female flies.

Several defining characteristics of virgin female flies help in sorting virgins from mated female flies. They include

1)Extremely pale body colour

2) meconium (waste products that remained after pupation) which appear as a dark spot near the abdomen

3)Folded wings

It is crucial to select virgin females as once the females have been inseminated, it stores the sperm in spermatheca and fertilizes the egg later. Hence if the females have been inseminated with males of not our interest, offspring born will not be of the required genotype.

2.4 The Flipout technique: This technique allows temporal and spatial regulation of any transgene under the control of a UAS promoter. The expression of the Flippase protein, induced by a heat shock, leads to the recombination of two cis FRT sites flanking a sequence containing a stop of transcription. Following the stop codon deletion, Gal4 comes under the regulation of a ubiquitous promoter and drives the expression of any transgene located downstream of a UAS site (Figure 2.4.1). In function of the conditions (heat shock duration and temperature), clones of different sizes may be generated. To activate the expression of Flippase in lines, females undergo a heat shock for 30 minutes at 37.5°C.

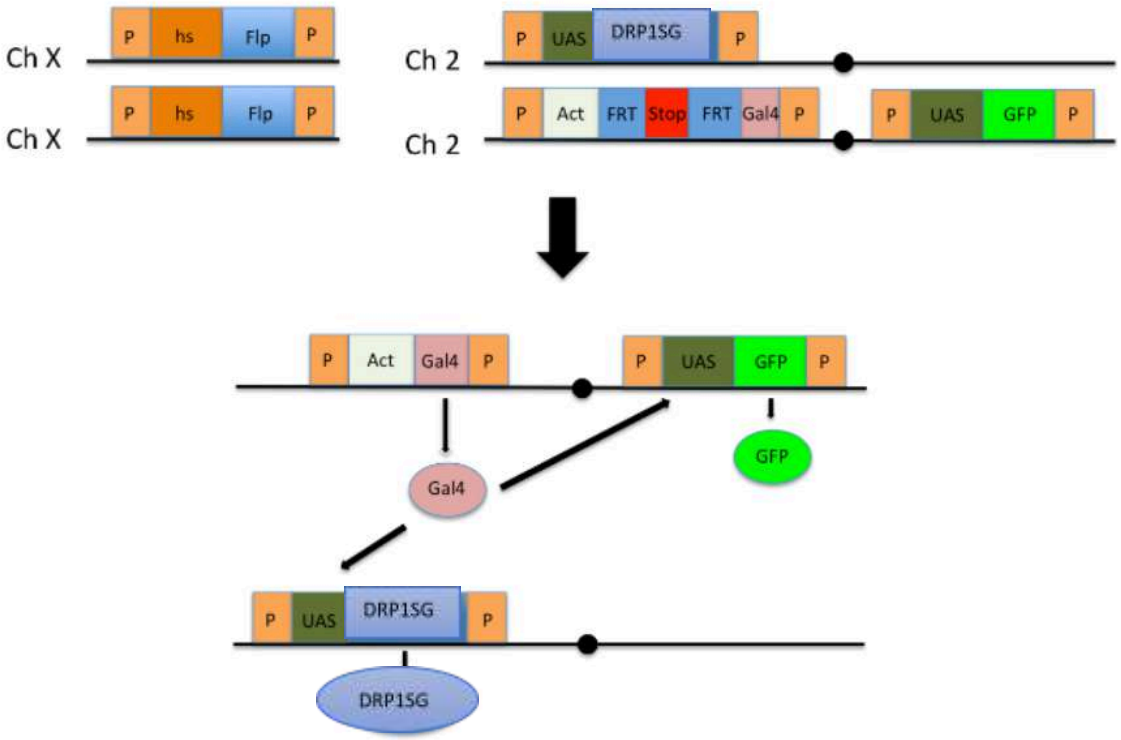

Figure 2.4.1. Schematic representation of the Flipout technique. The Flipout system enables inducible gene expression or clonal labeling through FLP recombinase-mediated excision of a stop cassette flanked by FRT sites. Upon FLP induction (e.g., by heat shock), the stop cassette is removed, activating downstream gene expression (e.g., GAL4), which in turn drives UAS-linked transgenes in marked cell clones. This allows spatial and temporal control of gene expression for lineage tracing or functional analysis.

2.5. Follicle staining for fixed imaging

Staining procedure

To perform staining of ovarian follicles, around ten young female flies are fed with yeast which improves their ovulation process and helps develop good ovaries fit for staining. After two days, around 5-6 flies are taken for dissection. The flies are put in ethanol for a few minutes, dried and are put in PBS. After dissection, the ovaries are transferred to a formaldehyde fixing solution (4% formaldehyde in PBS prepared just before dissection) and are incubated for 20 min at room temperature in rotation to fix them. After fixation, the ovarioles are given three washes in PBS and one wash in PBT. Afterwards, the ovarioles are incubated in a primary staining solution (400 µl of PBT and the required amount of antibody of interest) at 4°C overnight. After the overnight incubation, the ovaries are washed thrice in PBT, each for 30 minutes. They are incubated with a secondary staining solution (required amount of secondary antibody in 400µl of PBT) for 2 hours at room temperature in rotation. Afterward, the ovaries are washed with PBT, 4 times each for 15 minutes. Following the wash, the ovarioles are transferred to a slide, the follicles are separated from each other, and

mounted in antifade mounting media. The flies are dissected three days after the heat shock. (Figure 2.5.1)

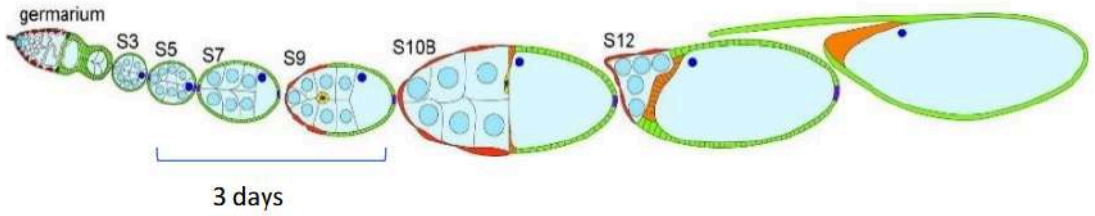

Figure. 2.5.1 The dissection is done three days after the heat shock so that the young follicles in which Flippase was activated would have reached stage 9.

2.6. Mitochondrial membrane potential CMXRos assay

CMXRos (Molecular Probes) (100 nM) in Schneider's medium was added to ovaries for 30 min and washed thrice in Schneider's medium for 5 min each. Fixation was done in 4%PFA in PBS for 15 min. The experiments for control and mutant samples used the same CMXRos dye aliquot, were done at the same time and imaged on the same day. To quantify mitochondria specific CMXRos signal, a thresholded mask was created based on the mitoGFP signal in ImageJ and was applied to the CMXRos channel, with excitation wavelength around 578 nm and an emission wavelength around 598 nm. CMXRos fluorescence was compared using non-parametric Mann Whitney test for statistical analysis.

2.7. Primary and secondary antibodies

The following antibodies and dyes are used:

- Primary Antibodies: Drp1 1°Ab , Marf 1°Ab, Mouse-Phosphotyrosine, Rat anti-Ecad (1:200), Mouse anti-Coracle 5 and 6 (1:50), Mouse anti-Dlg (1:50).
- Secondary Antibodies: Donkey anti Rat Min Cy5 (Ecad), Donkey anti Mouse Min Cy3 (Dlg+ Cor)
- Dye: Streptavidin 488, Phalloidin Alexa 647 ,Hoechst 33258, CMXRos

2.8. Mitochondrial morphology analysis

Fixed samples were imaged at RT using Zeiss confocal microscope (Zeiss Microsystems, Inc.; IISER Pune microscopy facility) with a Plan apochromat 100x oil-immersion objective. In the software, the images were acquired at 1024x1024 pixels. Fluorescent intensity was adjusted to avoid under- and oversaturation. Line averaging was set to 2 and acquisition speed to 200. The 406 diode laser line was used to excite the Alexa Fluor 488.

2.9 Image acquisition

The ovaries were imaged using a Plan apochromat 40× 1.3/1.4 NA objective on Zeiss LSM 710/780 nm. The images were grabbed with an averaging of 4 at 512 × 512 pixels. The laser power was kept similar between samples and the gain varied between 800–850 nm for antibody staining and 600–650 for CMXRos experiment. The range indicator mode was used for acquisition of each image so that the intensity did not reach 255 on an 8-bit scale. An ROI of 5–30 cells across an optical plane was chosen in each cell. Cytoplasmic signal and intensity was measured using ImageJ. Confocal images were acquired using AxioObserverZ1 LSM800 inverted confocal microscope with 40x and 63x objectives at the Platim, SFR Bioscience Lyon.

2.10. Quantification of E-cadherin in clones

To quantify and compare the expression of apical Ecad in mutant clones and wild-type cells, 5 Z stack images in each of the S7, and S9 stages having clones towards the anterior region of the follicle is acquired. Once the images are acquired, a z projection of the stack is generated using the Maximum parameter. The first image slice in the stack that shows the highest Ecad expression in the cell of our interest compared to the preceding slides to the slice at which the Ecad expression in the cell of our interest disappears are taken to generate the Z projection. This method of image slice selection to generate the Z stack is followed as Ecad expression is highest in the apical region compared to the basal and lateral domain of the cell. Due to the same reason, the maximum parameter is used instead of the average parameter as the maximum projection algorithm selects the pixels of the maximum intensity in every image selected to make a Z projection so that the final Z projection obtained will be a representation of Ecad in the apical domain of the cell of our interest. Once the Z stack is generated, the Ecad expression in the apical AJ of adjacent mutant and in the same column is quantified. All the quantifications are performed by drawing square ROI on the membrane of mutant/wild type cells shared by cells of the same genotype of our interest using Image J.

Chapter 3

RESULTS

3.1. Analysis of mitochondrial morphology and function in epithelial cell shape transition in follicle cells from cuboidal to squamous

To investigate the role of mitochondria in ovarian follicle cells when they undergo cell shape changes and flattening of St C, we tried comparing different stages of the follicles. We tried to check the pattern of mitochondria distribution in both anterior and posterior regions of cells once in early stage 7 (ES7) when the cell shape change had not started yet. (Figure 3.1.1) The other in early stage 9 (ES9), when the flattening of St C is seen and the anterior cells have transitioned from Cuboidal to squamous cells. We observe that in stage 7, there is no particular difference in mitochondria surrounding the nucleus in the anterior and posterior region. There was no difference in mitochondrial intensity in stage 7 and stage 9. However, differences in distribution of mitochondria is seen in wild-type follicles in S9. (Figure 3.1.2) In the anterior region we notice that mitochondria are present surrounding all over the nucleus in a circular pattern. Whereas in the central region where there is no cell shape change occurring and cells are columnar in shape, there mitochondria are present around the nucleus in crescent shape and not all over.

To compare mitochondrial membrane potential in anterior region as compared to posterior region, the ovaries were stained with CMXRos and imaged to study the changes in the dynamics of mitochondrial potential, nucleus and plasma membrane. In *Drosophila* ovaries during oogenesis, it can be seen that ovarian follicle cells present in the anterior region have more mitochondrial potential which can be visualized with the CMXRos high intensity. The mitochondrial distribution is less in the posterior region as compared to the anterior.

To study if higher membrane potential is there when cells undergo flattening, comparison was done between early stage 7(ES7) & and early stage 9(ES9) follicles stained with CMXRos dye. No difference seen in membrane potential between anterior and posterior region of cells in ES7 (Figure. 3.1.3). For Stage9, quantification shows significant increase in membrane potential intensity in the anterior region where cells are stretching as compared to posterior. As stretching of cells is an active process more mitochondrial activity in the anterior region is required. Thus increased mitochondrial activity is seen in stretching cells in the anterior

region where cell shape changes from cuboidal to squamous. (Figure 3.1.4)

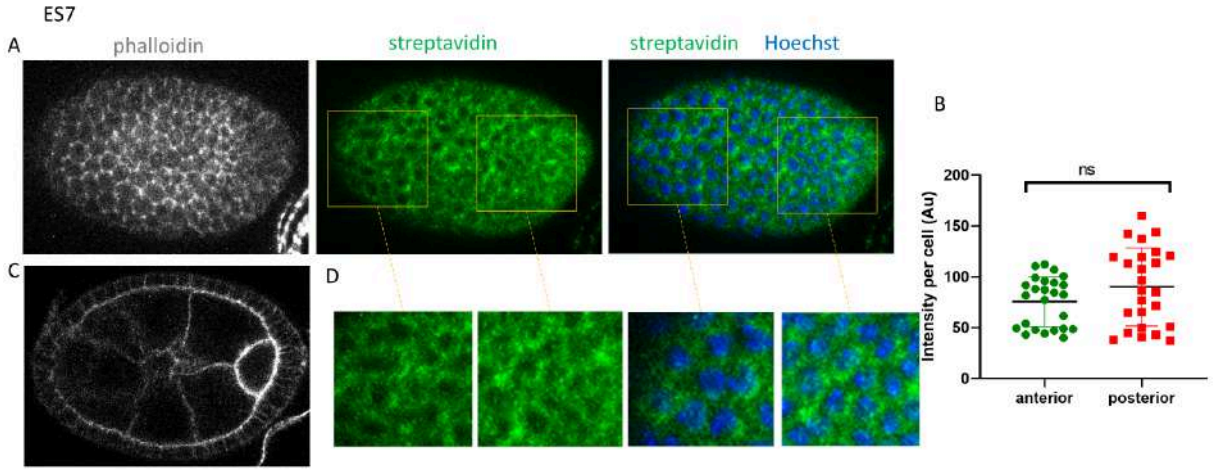

Figure 3.1.1: Mitochondrial distribution in ovarioles at early stage 7. No particular difference in mitochondria surrounding the nucleus in the anterior and posterior region. A. Confocal microscopy images showing early stage 7 of wild-type ovarian follicle cells. B. Quantification showing difference in mitochondrial intensity between anterior and posterior cells (n=5), 5 cells from anterior, 5 posterior for 5 different follicles was taken. Non parametric Mann-Whitney test was used for statistical analysis. ns. Non significant ($p > 0.05$). C. Full length sagittal view of the ovary. D. Zoomed in cells showing a similar pattern of mitochondria all around the nucleus in both anterior and posterior cells. S7: Stage 7

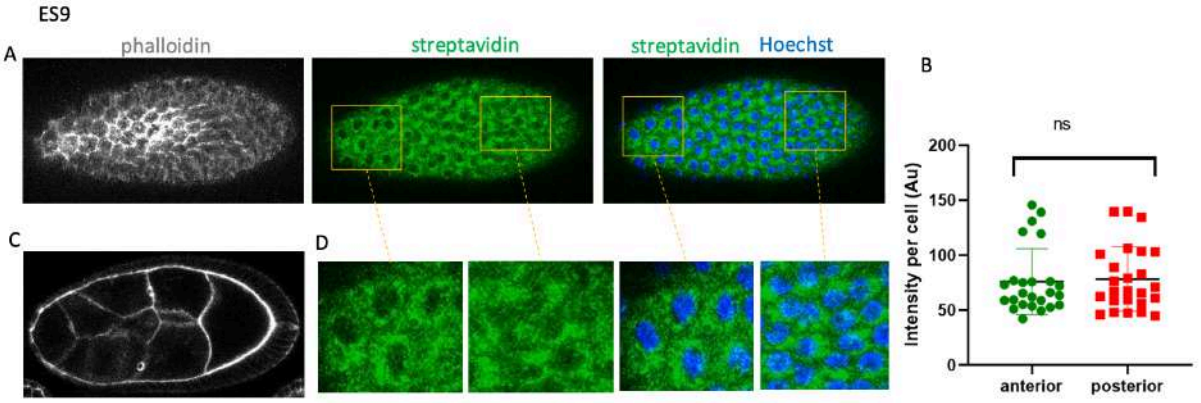

Figure 3.1.2: Mitochondria distribution in ovarioles in stage 9 A. Confocal microscopy images showing stage 9 of wild-type ovarian follicle cells. B. Quantification showing difference in mitochondrial intensity between anterior and posterior cells (n=5), 5 cells from anterior, 5 posterior for 5 different follicles was taken. Non parametric Mann-Whitney test was used for statistical analysis. ns. Non significant ($p > 0.05$). C. Full length sagittal view of the ovary. D. Zoomed in cells showing a difference in pattern of mitochondria localization all around the nucleus in anterior and one-sided crescent like pattern in posterior cells. ES9: Early Stage 9

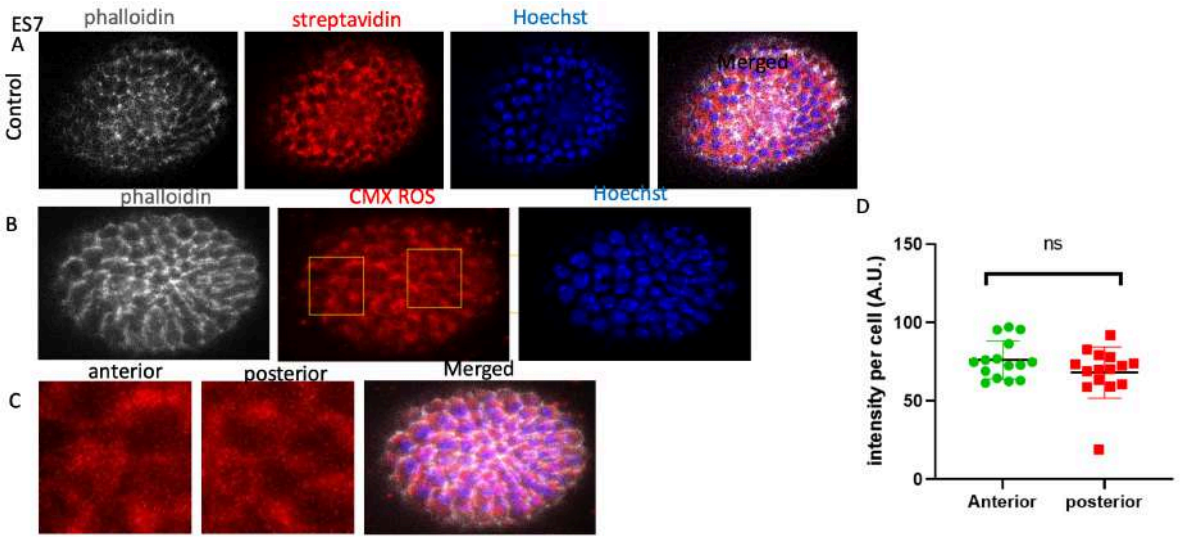

Figure 3.1.3: Mitochondrial membrane potential in stage 7 anterior flattened cells and posterior columnar cells. 3.1.3.A. Visualisation of ES7 wild-type ovarian follicle cells showing membrane, mitochondria, nucleus and their merged image. B. Similar stage 7 wild-type follicle stained with CMXRos dye is shown. C. To compare the intensity of membrane potential, zoomed in sections of anterior and posterior is shown. D. Quantification of mitochondrial intensity (5 cells from anterior, 5 posterior) for n=3 follicles shows similar potential in anterior and posterior region in S6. Non parametric Mann Whitney t test was done. ns: non significant .
P> 0.05

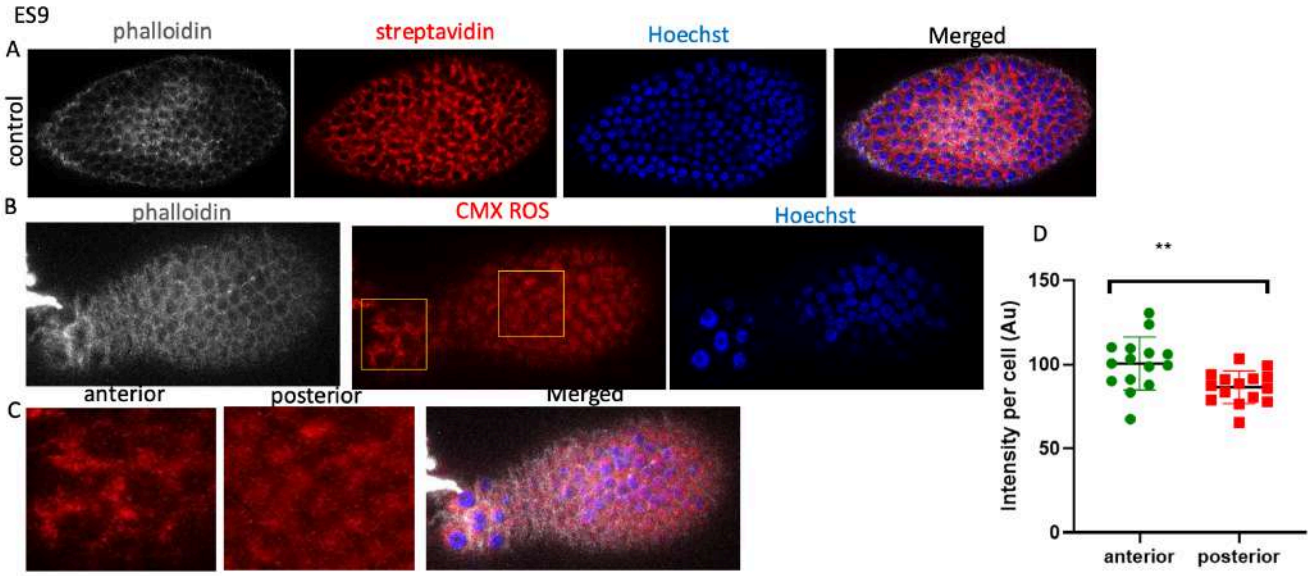

Figure 3.1.4: Mitochondrial membrane potential in stage 9 anterior flattened cells and posterior columnar cells. 3.1.2.A. Visualisation of ES9 wild type ovarian follicle cells showing membrane, mitochondria, nucleus and their merged image. B. Similar stage 9 wildtype follicle stained with CMXRos dye is shown. C. To compare the

intensity of membrane potential, zoomed in sections of anterior and posterior is shown. D. Quantification of mitochondrial intensity (5 cells from anterior, 5 posterior) for n=3 follicles shows significantly higher intensity of potential in anterior compared to posterior. Non parametric Mann Whitney t test was done. P value summary: ** . P<0.05

3.2. Alteration of mitochondrial distribution in mitochondrial fission and fusion depleted nurse cells and its impact on follicle cell organization

We expressed dominant negative mutant for Drp1, Drp1^{SG} and Marf RNAi in germ cells to deplete the mitochondrial fission and fusion activities, respectively. We made crosses with *nanos*-mito::GFP-GAL4 which specifically expresses in nurse cells. We first tested if expression of the Drp1^{SG} and Marf RNAi caused changes in mitochondrial organization. We see striking differences in the way mitochondria are localized in the DRP1^{SG} mutant nurse cells, when crossed with *nanos*-mito::GFP-GAL4 (Figure 3.2.1) Here we see patches of mitochondria clustered to only one side of the nucleus. Whereas in wildtype nurse cells, the mitochondria are localized all around the nucleus. The nucleus sizes in mutant cells are also irregular, some extremely big and some very small. Unlike wildtype ones, where there is uniformity in nucleus size. Mutant cells look irregular and stretched as compared to wild-type ones which are uniform and similar to one another. This was seen in 3 follicles of the same stage.

Defects seen in the way mitochondria are localized in the Marf1 RNAi mutant nurse cells. (Figure 3.2.2) In the case of Marf1 RNAi mutant cells, where fusion is perturbed and only fission is taking place, we see fragments of mitochondria all over the cell and not specifically around the nuclear region, when crossed with *nanos*-mito::GFP-GAL4 which specifically expresses in nurse cells. Whereas in wildtype germ cells, the mitochondria are accumulated all around the nucleus. Not much difference in nucleus size was observed in mutant cells. We notice uniformity in nucleus size and cell shape and size in mutant cells just like the control ones. This was seen in 3 follicles of the same stage 9.

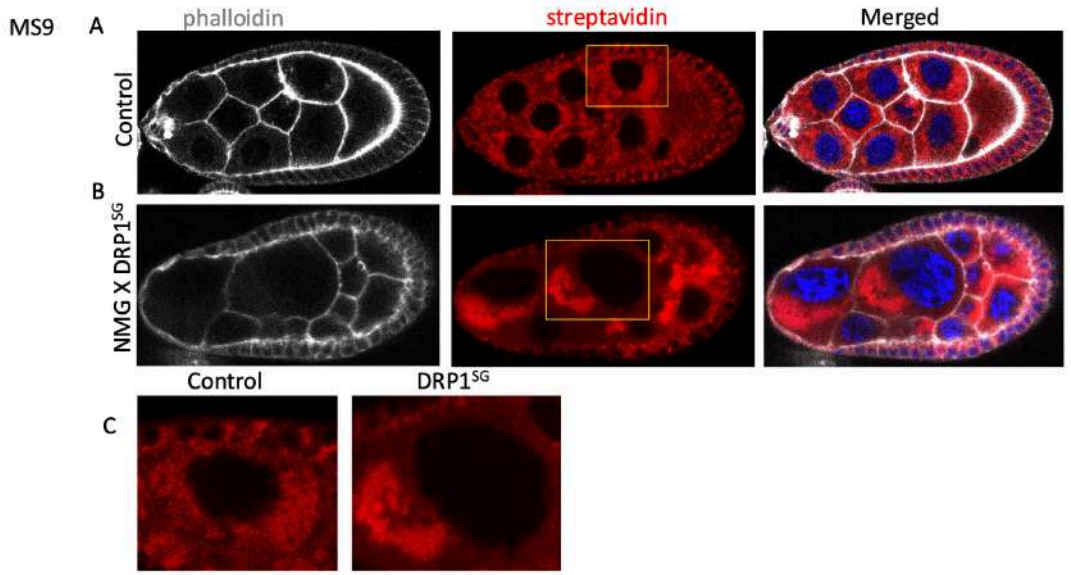

Figure 3.2.1 Alteration of mitochondrial distribution in mitochondrial fission depleted nurse cells A. Confocal microscopy images showing mid stage 9 of wild type ovarian follicle cells B. Visualisation of late stage 9 *nanos*-mito::GFP-GAL4 X DRP1^{SG} Cross follicle cells where mitochondria is clustered to one side of the nucleus. C. Zoomed in images of sections of wildtype germ cells and *nanos*-mito::GFP-GAL4 X DRP1^{SG} cross mutant cells comparing their mitochondrial distribution around nucleus is shown. MS9: Mid Stage 9

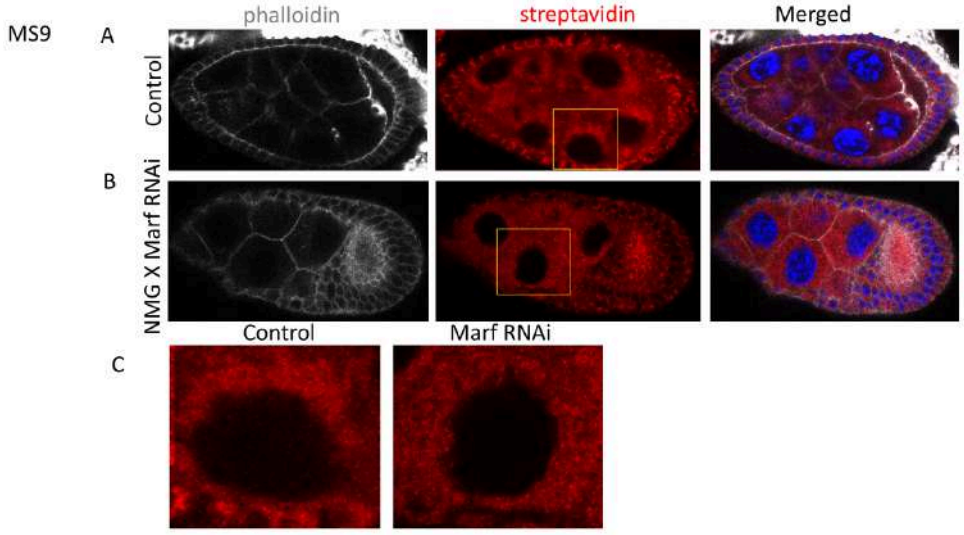

Figure 3.2.2 Alteration of mitochondrial distribution in mitochondrial fission depleted nurse cells. A. Confocal microscopy images showing mid stage 9 of wild type ovarian follicle cells where it is observed that mitochondria is present all around the nucleus uniformly. B. Visualisation of late stage 9 *nanos*-mito::GFP-GAL4 X Marf1 RNAi Cross follicle cells where fragments of mitochondria are seen all around the nucleus. C. Zoomed in images of sections of wildtype germ cells and *nanos*-mito::GFP-GAL4 X Marf RNAi cross mutant cells comparing their mitochondrial morphology around the nucleus is shown. MS9: Mid Stage 9

Drp1^{SG} expression leads to clustering of mitochondria in nurse cells but no defect in the follicle cells

Now as we have seen that DRP1^{SG} mutant is causing defects in nurse cells, we now want to see if causing a defect in nurse cells causes defects in follicle cells or not. To reveal mechanisms by which mitochondrial activity and metabolism regulate key interactions between germline and follicle cells for morphogenetic events in developmental processes. We wanted to check if perturbing the mitochondrial fission protein DRP1 in germline cells has an effect in follicle cells. In order to know that, DRP1^{SG} mutant flies were crossed with *nanos*-Gal4, Mito-GFP which expresses in germ cells. Here the germ cells were perturbed but we do not see any defect in follicle cells. (Figure 3.2.3)

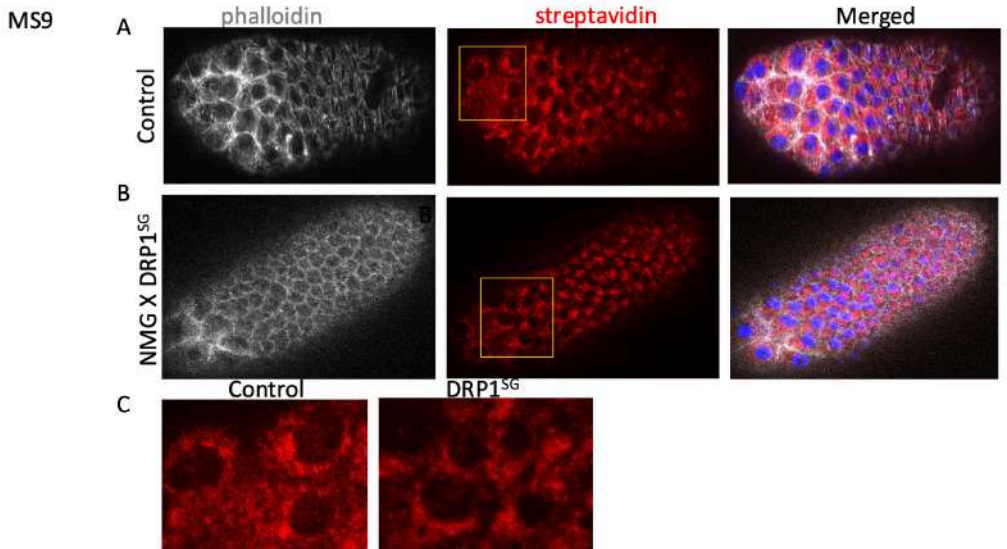

Figure 3. 2. 3: Drp1^{SG} expression leads to clustering of mitochondria in nurse cells but no defect in the follicle cells A. Confocal microscopy images showing mid stage 9 of wild type ovarian follicle cells B. Visualisation of late stage 9 *nanos*-mito::GFP-GAL4 X Drp1^{SG} Cross follicle cells. C. Zoomed in images of wildtype anterior cells and *nanos*-mito::GFP-GAL4 X DRP1^{SG} cross mutant cells comparing their mitochondrial morphology around nucleus is shown MS9: Mid Stage 9

Marf RNAi expression leads to more dispersed mitochondria in nurse cells but no defect in the follicle cells

To reveal mechanisms by which mitochondrial activity and metabolism regulate key interactions between germline and follicle cells for morphogenetic events in developmental processes. It is important to check if perturbing the mitochondrial fusion protein Marf1 RNAi in germline cells will have an effect in follicle cells. In order to study that, Marf1 RNAi mutant flies were crossed with Nanos Mito GFP which expresses in germ cells. Here the germ cells were perturbed i.e, only fission is being carried out in the germ cells and we do see dispersed mitochondria in nurse cells but no defect in the follicle cells observed in control flies. Hence not much difference in mitochondrial distribution. (Figure 3.2.4)

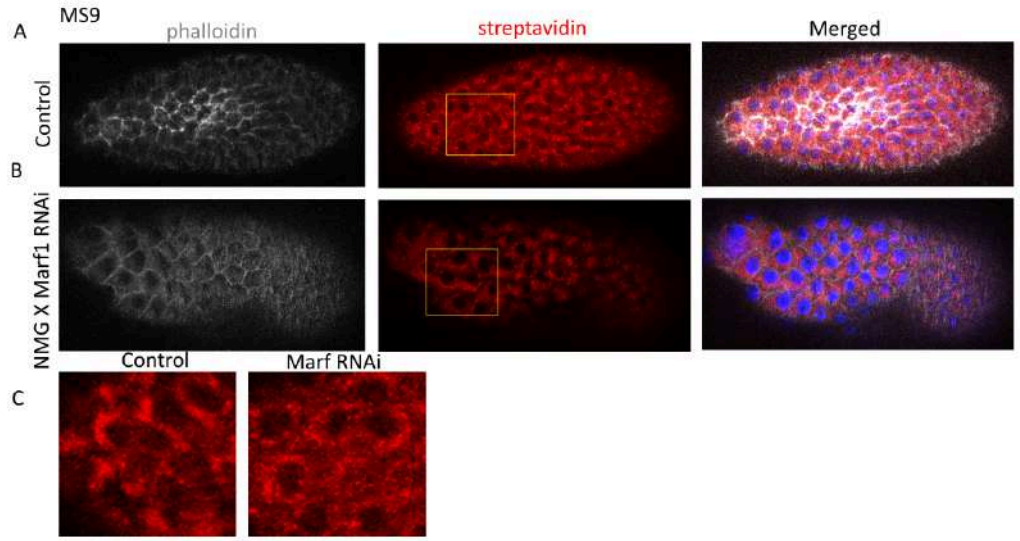

Figure 3.2.4. Marf RNAi expression leads to more dispersed mitochondria in nurse cells but no defect in the follicle cells A. Confocal microscopy images showing mid stage 9 of wild type ovarian follicle cells B. Visualisation of late stage 9 *nanos*-mito::GFP-GAL4 Marf1 RNAi Cross follicle cells. C. Zoomed in images of wildtype anterior cells and *nanos*-mito::GFP-GAL4 X Marf RNAi cross mutant cells comparing their mitochondrial morphology around the nucleus is shown. MS9: Mid Stage 9

Expression of Drp1^{SG} and Marf RNAi in germ cells does not cause a defect in follicle cell shape and nuclear size

Quantification done in S9 DRP1^{SG} follicle cells show an increase in nuclear size, cell membrane area and mitochondrial intensity when germ cells are perturbed as compared to control but the increase in all of them is non-significant. (Figure 3.2.5)

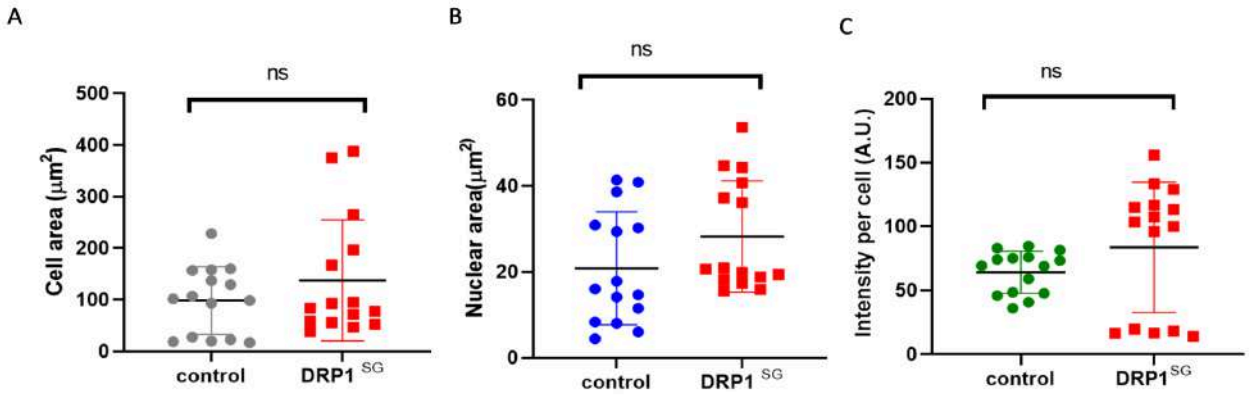

Figure 3.2.5. Quantification was done for the same set of MS9 wild follicle cells and DRP1^{SG} mutant follicle cells. No significant change was observed. A. Cell area of DRP1^{SG} mutant anterior cells (n=3), 5 cells each from WT and mutant cells for 3 different follicles of the same stage was compared to wild type follicle cells. There is an increase in cell area of the mutant cells however the difference is non significant. B. Increase in nuclear area was observed for the DRP1^{SG} mutant cells but the difference in nuclear size is non significant. C. Mitochondrial intensity is also plotted to understand better the accumulation of mitochondria in DRP1^{SG} mutant cells to wildtype, where the mutant cells show an increase. But again, the increase is not significant. Non parametric Mann-Whitney test was used for statistical analysis. ns. Non significant ($p > 0.05$).

Quantification done in S9 Marf RNAi follicle cells show an increase in nuclear size, cell membrane area and mitochondrial intensity when germ cells are perturbed as compared to control but the increase in all of them is non-significant. (Figure 3.2.6)

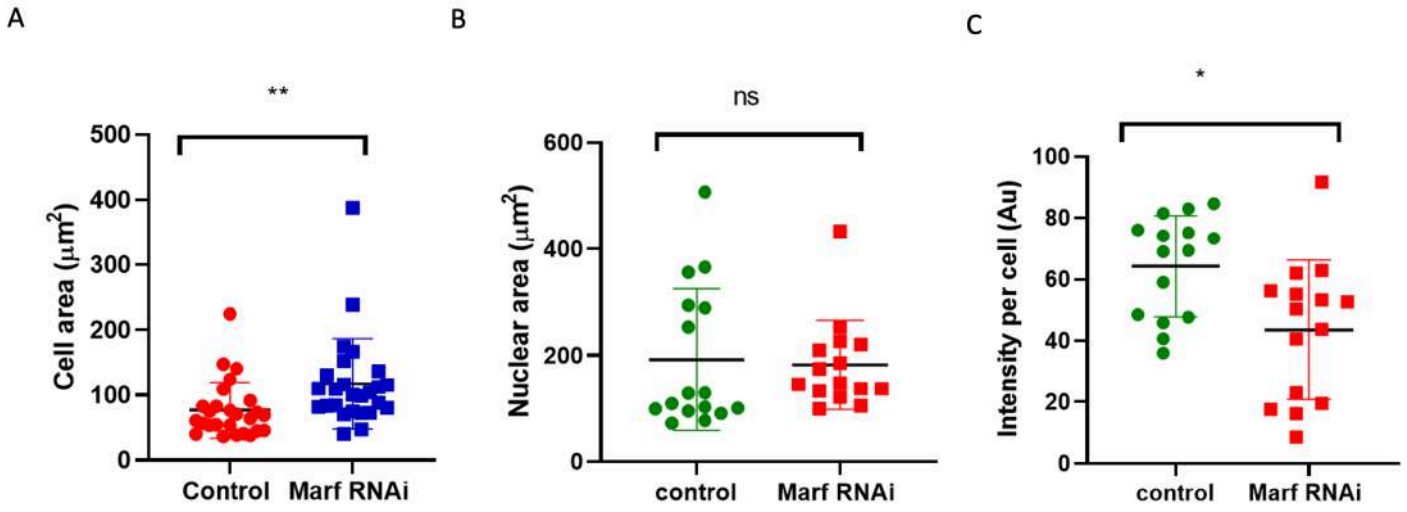

Figure 3.2.6. A. At MS9,Cell area of Marf1 RNAi mutant anterior cells (n=3), 5 cells each from WT and mutant cells for 3 different follicles of the same stage was taken and compared to wild type follicle cells. Increase in cell area of the mutant cells was noticed. Non parametric Mann-Whitney test was used for statistical analysis. P value summary: **($p < 0.05$). B. No difference in nuclear area was observed for the Marf1 RNAi mutant cells. Non parametric Mann-Whitney test was used for statistical analysis. Ns non significant ($p > 0.05$). C. Mitochondrial intensity is also plotted to understand better the distribution of mitochondria in Marf RNAi mutant cells to wild-type. Non parametric Mann-Whitney test was used for statistical analysis. P value summary: * ($p < 0.05$).

3.3. Analysis of defects in follicle cells on depletion of mitochondrial fusion and fission proteins in follicle cells

Clustered mitochondrial distribution around nucleus observed in DRP1^{SG} mutant when expressed in follicle cells

In order to test the change in mitochondrial distribution and activity during the cuboidal to squamous cell shape transition, we checked the effect of disruption of mitochondrial fission and fusion proteins, we used RNAi to deplete mitochondrial fission protein DRP1 and mitochondrial fusion protein Marf1. We used RNAi against complex I and IV subunits to deplete the mitochondrial electron transport chain activity. Mutant flies were crossed with GR-Gal4 which specifically expresses in follicle cells. Upon depletion of mitochondrial fission protein Drp1, we observed a difference in mitochondrial accumulation pattern in the anterior part as shown in figure. 3.3.1 Additionally, to address whether the disruption of Drp1 protein has any morphological effect, we observed that the cells were much more elongated compared to the control.

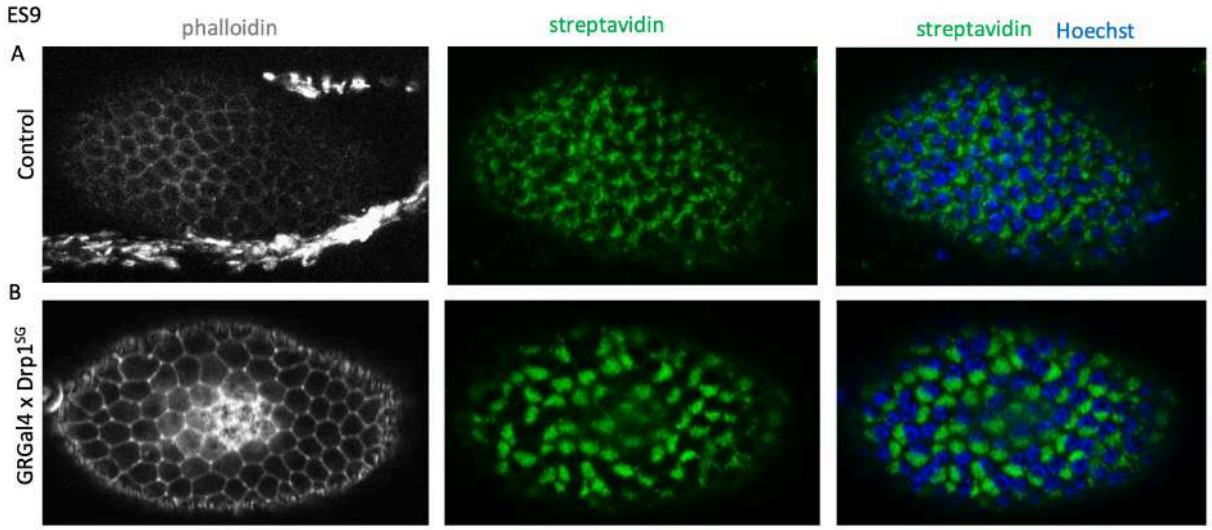

Figure 3.3.1. Clustered mitochondrial distribution around nucleus observed in DRP1^{SG} mutant when expressed in follicle cells A. Visualization of ES9 w^{1118} ovarian follicle cell. Here in the streptavidin panel, we observe that mitochondria is all around the nucleus. B. Visualization of ES9 follicle cell of DRP1^{SG} X GRGAL4 Cross flies. Clustered mitochondria around the nucleus in DRP1^{SG} mutant was observed. ES9: Early stage 9

Crosses were made with Marf RNAi mutant flies and Comp1 ND-51 sub unit flies with GR-GAL4 to check for differences in mitochondrial morphology as compared to control. Both of these two crosses led to lethality and hence the ovarioles could not be analyzed.

Clonal analysis of epithelial defects in follicle cells depleted for Drp1 and Marf

Clonal expression of Drp1^{SG} in follicle cells shows a decrease in cell area as compared to neighbouring control follicle cells

Crosses of Drp1^{SG} mutant flies X *hs-Flp*;Act-FRTstopFRTGal4, UAS-GFP/CyO were made. This was to test their role in the Stretched cells for their shape. Here I could compare the clonal mutant cells and the wild-type cells in the same follicle. Our goal here was to visualize how mitochondria look like when it is perturbed as compared to wildtype. We could see fused mitochondria in the anterior region of cells. And compare these cells with the adjacent wild type ones. (Figure 3.3.2) Although follicles having clustered mitochondria were less in the anterior region in the stage where cells are stretching, still n=4 follicles were quantified. DRP1^{SG} mutant cells with fused mitochondria have smaller cell area as compared to control cells. Whereas, the nuclear area is bigger for mutant cells which is non-significant. We tried doing the same thing twice, once only taking those DRP1^{SG} mutant clones which had fused mitochondria and the other set by comparing overall DRP1^{SG} clones not just the ones with fused mitochondria. For the first set, the membrane marker used was M- Phospho tyrosine and for the second one Ecad. So we wanted to compare both the

Cadherin and Phosphotyrosine levels to study epithelial cell remodeling.

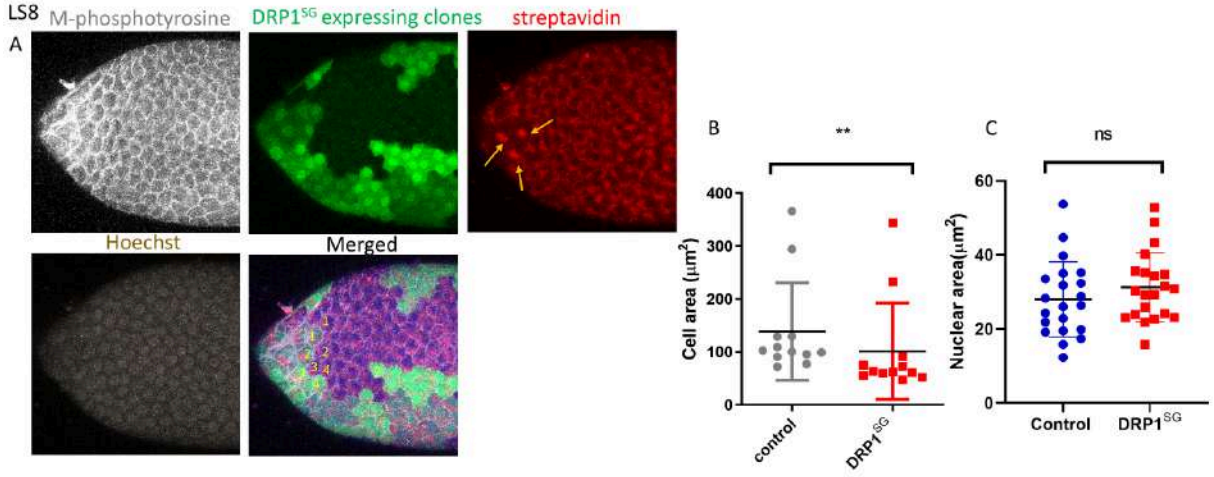

Figure 3.3.2. Clonal expression of Drp1^{SG} in follicle cells with fused mitochondria. A. Visualization of LS8 ovarian follicle cell where wild-type and DRP1^{SG} expressing clones are seen in the same follicle A. M-phosphotyrosine is marking the cell membrane. In the streptavidin panel, pointed arrows are marking the clonal DRP1^{SG} cells where the mitochondria is fused in the anterior region. In the merged section, the wild-type and the adjacent DRP1^{SG} mutant cells are marked as (1,1) , (2,2) in a wave-like manner till 4 cells. LS8: Late stage 8. B. Non parametric Mann-Whitney test was used for statistical analysis. P value summary : **. P < 0.05. C. Nuclear area of DRP1^{SG} expressing cells with fused mitochondria was almost similar to wildtype (4,4) cells of each wildtype and clones were taken for 4 different follicles, the same used for quantifying cell area. Non parametric Mann-Whitney test was used for statistical analysis. ns. Non-significant. P > 0.05.

Quantification shows a decrease in cell area of DRP1^{SG} clonal cells where mitochondria is fused as compared to wildtype. Not much difference in nuclear area was found. (Figure 3.3.4)

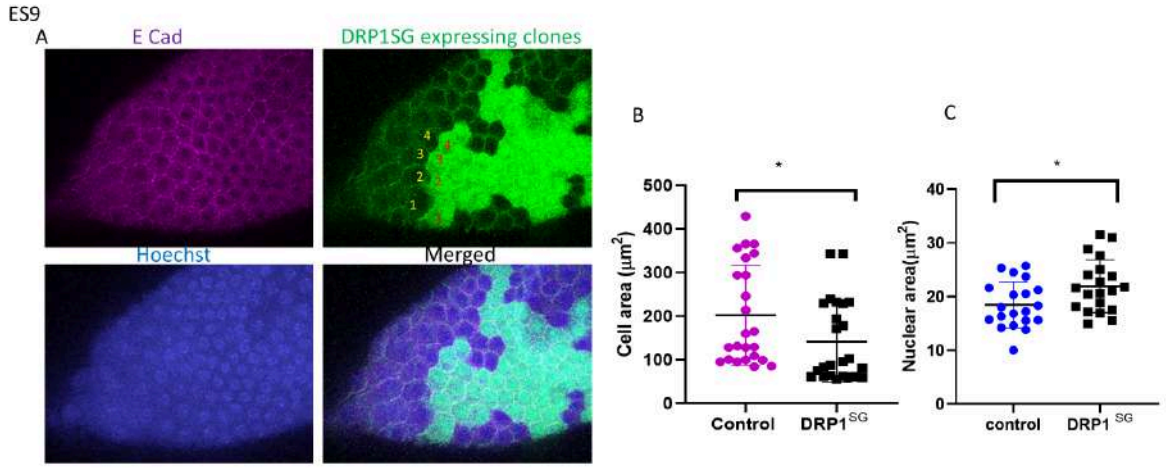

Figure 3.3.4. Visualization of ES9 ovarian follicle A. In the GFP panel, DRP1^{SG} clone cells and their adjacent wildtype cells are denoted as (1,1), (2,2) in the anterior region for n= 5 follicles. Cell area of DRP1^{SG} expressing cells with fused mitochondria is smaller as compared to wildtype, (4,4) cells for n=5 follicles. Non parametric Mann-Whitney test was used for statistical analysis. P value summary : *. P < 0.05. C. Nuclear area of DRP1^{SG} expressing cells is bigger in size compared to wildtype (4,4) cells for n=5 follicles. Non parametric Mann-Whitney test was used for statistical analysis. P value summary: * P < 0.05. ES9:Early Stage 9

We wanted to compare the Ecad level and Phosphotyrosine levels for both control and DRP1 ^{SG} mutant cells. DRP1^{SG} adherens junctions seems to remodel earlier but it is not consistent always. (Figure 3.3.5)

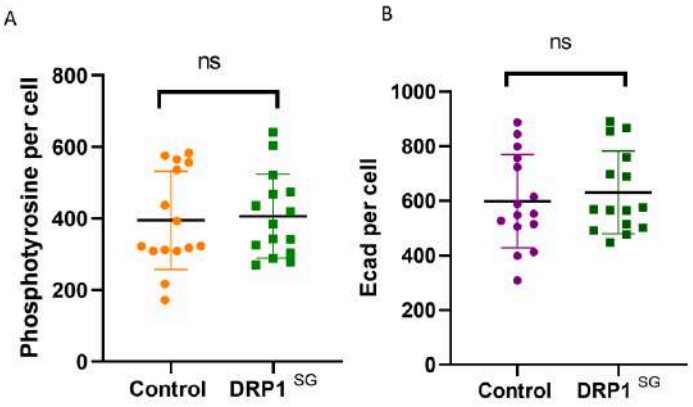

Figure 3.3.5. A. Phosphotyrosine and E cadherin levels for control and DRP1 ^{SG} were quantified. Non parametric Mann-Whitney test was used for statistical analysis. Ns: non significant. B. In DRP1^{SG} cells, Ecad level is higher compared to control but not consistent. Non parametric Mann-Whitney test was used for statistical analysis. Ns: non significant

Clonal expression of Marf RNAi in follicle cells shows an increase in cell area as compared to neighbouring control follicle cells

Marf RNAi expressing clones are bigger in cell area as compared to adjacent control cells, whereas their difference in nuclear area is nonsignificant. (Figure 3.3.6)

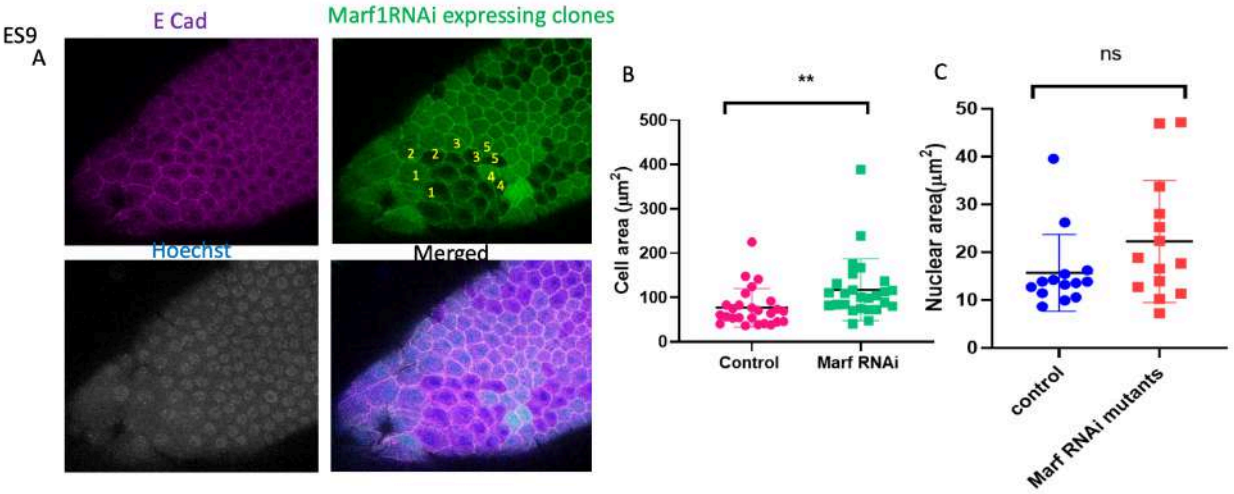

Figure 3.3.6. Visualization of ES9 ovarian follicle cell where wildtype and Marf RNAi expressing clones A. In the GFP panel, Marf RNAi clone cells and their adjacent wildtype cells are denoted as (1,1), (2,2) in the anterior region for n= 5 follicles. B. Cell area of Marf1 RNAi expressing cells is bigger as compared to wildtype, (4,4) cells for n=5 follicles. Non parametric Mann-Whitney test was used for statistical analysis. P value summary : **. P < 0.05. C. Nuclear area of DRP1SG expressing cells is bigger in size compared to wildtype (4,4) cells for n=5

follicles, but the difference is non-significant. Non parametric Mann-Whitney test was used for statistical analysis. ns: non significant P > 0.05.

3.4. Impact of mitochondria fission fusion proteins in remodelling of epithelial polarity proteins

DRP1^{SG} cells start early remodelling of Adherens junctions compared to wild-type

To comment on the cell remodelling of Adherens junctions and check if mitochondria have a role to play in it, DRP1^{SG} mutant flies were crossed with *hs-Flp*; Act-FRTstopFRTGal4, UAS-GFP/CyO. Here E cad levels are being looked at to comment on disassembly of Adherens junction. In this system, we are able to compare the E cad levels in mutant and adjacent wild types. AJ is defined as continuous if the membrane it resides on has no gaps and discontinuous if it has several gaps in between. The continuous and discontinuous nature of the cell membrane can be considered as a representation of the AJ's localization and distribution.

To assess whether AJ responds to a depletion of DRP1^{SG} fission protein by reducing the Ecad expression, we checked the Ecad expression in wild-type for various controls in early stage 7 and stage 9 columnar and stretched cells. Preliminary results show that, due to the difference in Ecad expression between wild-type and DRP1^{SG} expressing clones, DRP1^{SG} clonal cells seem to have disassembled earlier in the S9 stage. This analysis is still undergoing.

Comparison was done based on discontinuity and continuity of AJ in S9 where cells are undergoing flattening of St-C (Figure 3.4.1) In this stage, we wanted to see which cells were remodeling earlier by looking at the Ecad expression**.** Although the cells might have started the remodeling processes not at the same time, but at one level when cells are stretching DRP1^{SG} mutant cells seem to have undergone remodeling earlier as compared to wildtype, where the adherence junctions are still intact.

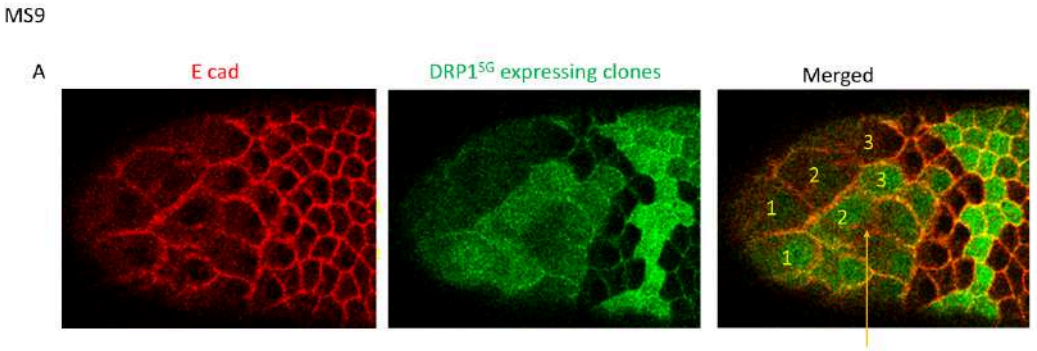

Figure 3.4.1. A. Confocal microscopy images of Early Stage 9 ovarian follicle cell to show comparison of the cell remodelling occurring in DRP1^{SG} expressing clones to wildtype cells. In the GFP Panel, cells are marked as (1,1), (2,2), (3,3) one for the DRP1^{SG} expressing clones and other their adjacent wildtype ones. B. Zoomed in the section of E Cad staining in the anterior region is shown. M: Mutant cell, W: wild-type. Here We observe that in the section pointed with an arrow which are mutant cells, the adherence junction is disassembling and

discontinuous and has gaps. Whereas in the adjacent wild type cell the adherence junction is still intact. n=3 follicles.

Delayed remodelling of Marf RNAi cells of Adherens junctions compared to wild-type

In this case, we wanted to see if depleting mitochondrial fusion protein Marf1 has an effect on cell shape remodeling during S9 where cells undergo cell shape change and flattening of StC.
Crosses of Marf1 RNAi with *hs-Flp*; Act-FRTstopFRTGal4, UAS-GFP/CyO were made. E cad staining was looked at to comment upon the disassembly of Adherens junction. We notice that Marf RNAi expressing clonal cells adherens junctions are still intact as compared to their adjacent wild-type which are disassembled (Figure 3.4.2) Whereas in the adjacent Marf RNAi clone cell the adherence junction is still intact. Although the cells might have started the remodeling processes not at the same time, but at one level when cells are stretching Marf1 RNAi mutant cells seem to have undergone delayed remodeling as compared to wild-type, where the adherence junctions are disassembled**.** This was observed in n=3 follicles. This is exactly opposite to what we see in $DRP1^{SG}$ clonal cells.

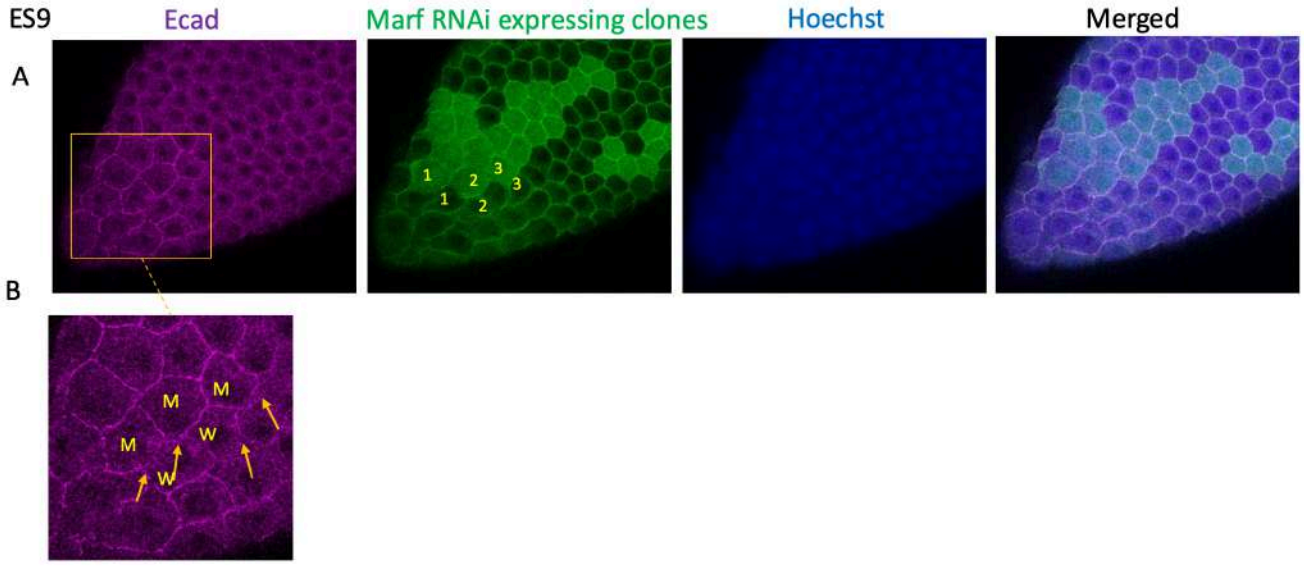

Figure 3.4.2. A. Confocal microscopy images of Early Stage 9 ovarian follicle cell to show comparison of the cell remodelling occurring in Marf RNAi expressing clones to wildtype cells. In the GFP Panel, cells are marked as (1,1), (2,2), (3,3) one for the Marf RNAi expressing clones and other their adjacent wildtype ones. B. Zoomed in the section of E Cad staining in the anterior region is shown. M: Mutant cell, W: wild-type. Here We observe that in the section pointed with arrows which are wild type the adherence junction is disassembling and non discontinuous and has gaps. Whereas in the adjacent Marf RNAi clone cell the adherence junction is still intact. n=3 follicles.

Chapter 4

DISCUSSION

This study indicates mitochondrial dynamics and function regulates epithelial cell remodelling during *Drosophila* oogenesis. More specifically, depleting mitochondrial fission and fusion proteins in the germ cells causes defects hindering the regular development of ovarian follicle cells, which was evidently seen in the ovarian follicle. The $DRP1^{SG}$ and Marf RNAi mutants in germ cells lead to clustered and fragmented mitochondria respectively. Expression of $Drp1^{SG}$ and Marf RNAi in germ cells does not cause a defect in follicle cell shape and nuclear size. Expression of $Drp1^{SG}$ and Marf RNAi in follicle cells leads to decrease and increase in cell area respectively with an alteration of the stage of cell shape remodelling.

Mitochondrial Dynamics and Follicle Cell Shape Transition

Mitochondrial distribution was found to change during the transition of follicle cells from cuboidal to squamous morphology, particularly in the anterior region of stage 9 follicles. In wild-type cells, mitochondria were predominantly distributed in a circular pattern around the nucleus in squamous follicle cells, whereas columnar cells in the central region exhibited a crescent-like mitochondrial arrangement. This suggests that mitochondrial positioning is influenced by cell shape changes and may play an active role in supporting cytoskeletal reorganization during epithelial flattening.

The increased clustering of mitochondria in squamous follicle cells at stage 9 could indicate a higher energy demand required for active cytoskeletal remodeling. Epithelial cell flattening is a dynamic process that requires ATP to fuel actin polymerization and myosin II contractility. Studies have shown that localized mitochondrial activity is essential for cytoskeletal organization, as ATP availability directly influences actin filament assembly and adhesion complex stability (Cunniff et al., 2016). The contrast between anterior and posterior follicle cells in mitochondrial localization further suggests that differential mitochondrial positioning reflects localized energetic demands during morphogenesis.

Atypical protein kinase C (aPKC) plays a crucial role in regulating cell polarity and cytoskeletal dynamics, particularly influencing the actomyosin complex. Research indicates that aPKC antagonizes myosin II-driven contraction of the actin cytoskeleton. Specifically, aPKC phosphorylates and inhibits Rho-associated kinase (ROCK), a key activator of myosin II. This inhibition prevents excessive myosin II activity, thereby modulating actomyosin contractility.

It is noted that a decrease in atypical protein kinase C (aPKC) leads to increased myosin activation, which in turn contributes to the constriction of follicle cells. Specifically, in follicle cells where the mitochondrial fission protein Drp1 is depleted, aPKC is lost from the apical membrane. This loss of aPKC is associated with an increased apical constriction of the follicle cells. Since aPKC is known to play a role in maintaining epithelial polarity and regulating cytoskeletal dynamics, its depletion disrupts normal polarity and enhances actomyosin contractility.

The increase in myosin activation is likely due to the loss of aPKC-mediated inhibition of the Rho-associated kinase (ROCK) pathway, which is a well-known regulator of myosin II activity.

When aPKC is present, it phosphorylates and inhibits components that promote myosin activity. However, in its absence, myosin II becomes hyperactivated, leading to increased actomyosin complex formation and enhanced contractility. This results in excessive apical constriction, a phenomenon observed in Drp1 mutant follicle cells.

Thus, the depletion of aPKC creates conditions that favor actin-myosin network assembly and contractility, reinforcing the idea that aPKC functions as a key regulator of cytoskeletal dynamics in epithelial cell polarity and tissue architecture.

Disrupting mitochondrial fission and fusion through the expression of dominant-negative $DRP1^{SG}$ and Marf RNAi in nurse cells did not lead to observable defects in follicle cell shape, nuclear size, or organization. This suggests that follicle cell remodeling is largely autonomous and not significantly influenced by germline mitochondrial perturbations. Germline cells supply nutrients and signaling molecules to the surrounding follicle cells, but the maintenance of epithelial integrity and remodeling may rely on cell-intrinsic metabolic pathways (Mitra et al., 2012). However, when $DRP1^{SG}$ was expressed directly in follicle cells, mitochondria became clustered around the nucleus, leading to a decrease in cell area. Conversely, Marf RNAi expression resulted in dispersed mitochondria and an increase in cell area. These observations suggest that mitochondrial morphology directly affects cell shape regulation, likely through modulating ATP production, cytoskeletal interactions, and mechanical forces within the cell.

Impact of Mitochondrial Dynamics on Adherens Junction Remodeling

One of the key findings of this study is the differential effect of mitochondrial fission and fusion on adherens junction (AJ) remodeling. $DRP1^{SG}$ mutant follicle cells displayed early remodeling of AJs, as evident from the earlier disassembly of E-cadherin in stage 9 follicles compared to wild-type cells. This suggests that mitochondrial fission may promote AJ turnover, potentially facilitating epithelial flattening. A possible explanation is that increased mitochondrial fission enhances ATP availability for cytoskeletal regulators involved in AJ remodeling, such as actomyosin networks. Studies have demonstrated that increased ATP production due to mitochondrial fission supports cytoskeletal contractility and adhesion turnover, particularly in migratory cells (Yang et al., 2014). This could explain why $DRP1^{SG}$ mutant cells exhibit premature AJ disassembly.

In contrast, Marf RNAi mutant cells exhibited delayed AJ remodeling, maintaining intact E-cadherin junctions longer than their wild-type counterparts. This delay in junctional remodeling correlates with the observed increase in cell area, suggesting that mitochondrial fusion may be necessary for the timely disassembly of AJs during epithelial remodeling. Mitochondrial fusion is typically associated with maintaining oxidative phosphorylation and overall mitochondrial function. Reduced mitochondrial fusion often leads to defects in ATP generation and an accumulation of dysfunctional mitochondria (Liesa & Shirihai, 2013). The delayed AJ disassembly observed in Marf RNAi cells may be due to reduced ATP production or inefficient ROS signaling, both of which could impair the cellular remodeling process.

Interestingly, quantification of mitochondrial membrane potential using CMXRos staining showed that mitochondrial activity was significantly higher in anterior follicle cells at stage 9 compared to posterior cells. This supports the hypothesis that mitochondrial function is

crucial for epithelial shape transitions, as actively remodeling cells require more energy to undergo cytoskeletal and adhesion rearrangements. High mitochondrial activity in remodeling cells has been reported in other developmental contexts, such as neural crest cell migration and epithelial-mesenchymal transitions (EMT), where cells require significant ATP production to facilitate changes in adhesion and motility (Rao et al., 2019).

Future Directions and Implications

Further investigations are needed to determine whether the observed changes in AJ remodeling are mediated by mitochondrial energy production, ROS signaling, or direct interactions with cytoskeletal components. Live imaging studies could provide insights into the real-time dynamics of mitochondrial positioning and AJ remodeling in follicle cells.

It would also be valuable to explore the role of mitochondrial distribution in other epithelial morphogenetic events, such as tissue elongation and invagination, to determine whether similar principles apply to different developmental contexts. Additionally, investigating the potential interaction between mitochondrial function and signaling pathways like Notch and TGF-β, which are known to regulate epithelial remodeling, could provide a more comprehensive understanding of the mechanisms at play.

Understanding the role of mitochondrial dynamics in epithelial remodeling has broader implications beyond *Drosophila* oogenesis. Epithelial morphogenesis is a fundamental process in development and disease, and mitochondrial dysfunction has been implicated in various pathological conditions, including cancer and fibrosis. Our findings highlight the need to explore mitochondrial dynamics as a regulatory mechanism in epithelial tissue organization and mechanical homeostasis.

In summary, our study demonstrates that mitochondrial fission and fusion differentially regulate epithelial cell shape and AJ remodeling in *Drosophila* follicle cells. While DRP1-mediated fission promotes AJ turnover and epithelial flattening, Marf-mediated fusion delays AJ remodeling and increases cell area. These findings suggest that mitochondrial dynamics play a crucial role in epithelial morphogenesis, potentially through modulating ATP production, cytoskeletal interactions, and junctional integrity. Further studies will be essential to uncover the precise molecular pathways linking mitochondrial function to epithelial remodeling.

Chapter 5

References:

Aguilar-Aragon, M., Bonello, T. T., Bell, G. P., Fletcher, G. C., & Thompson, B. J. (2020). Adherens junction remodelling during mitotic rounding of pseudostratified epithelial cells. *EMBO Reports*, *21*(4). https://doi.org/10.15252/embr.201949700

Balaji, R., Weichselberger, V., & Classen, A. K. (2019). Response of Drosophila epithelial cell and tissue shape to external forces in vivo. *Development (Cambridge)*, *146*(17). https://doi.org/10.1242/dev.171256

Brigaud, I., Duteyrat, J. L., Chlasta, J., Bail, S. le, Couderc, J. L., & Grammont, M. (2015). Transforming growth factor b/activin signalling induces epithelial cell flattening during drosophila oogenesis. *Biology Open*, *4*(3), 345–354. https://doi.org/10.1242/bio.201410785

Brouzés, E., & Farge, E. (2004). Interplay of mechanical deformation and patterned gene expression in developing embryos. In *Current Opinion in Genetics and Development* (Vol. 14, Issue 4, pp. 367–374). https://doi.org/10.1016/j.gde.2004.06.005

Carlier, M.-F., Pantaloni, D., & ¡ *-S Monomer, A. (1986a). *Biochemistry © Accelerated Publications Direct Evidence for ADP-Pi-F-Actin as the Major Intermediate in ATP-Actin Polymerization. Rate of Dissociation of Pi from Actin Filaments*. https://pubs.acs.org/sharingguidelines

Carthew, R. W. (2005). Adhesion proteins and the control of cell shape. In *Current Opinion in Genetics and Development* (Vol. 15, Issue 4, pp. 358–363). https://doi.org/10.1016/j.gde.2005.06.002

Chlasta, J., Milani, P., Runel, G., Duteyrat, J. L., Arias, L., Lamiré, L. A., Boudaoud, A., & Grammont, M. (2017). Variations in basement membrane mechanics are linked to epithelial morphogenesis. *Development (Cambridge)*, *144*(23), 4350–4362. https://doi.org/10.1242/dev.152652

Chowdhary, S., Madan, S., Tomer, D., Mavrakis, M., & Rikhy, R. (2020). Mitochondrial morphology and activity regulate furrow ingression and contractile ring dynamics in drosophila cellularization. *Molecular Biology of the Cell*, *31*(21), 2331–2347. https://doi.org/10.1091/mbc.E20-03-0177

Costa, M., Raich, W., Agbunag, C., Leung, B., Hardin, J., & Priess, J. R. (1998a). A Putative Catenin-Cadherin System Mediates Morphogenesis of the Caenorhabditis elegans Embryo. In *The Journal of Cell Biology* (Vol. 141, Issue 1). http://www.jcb.org

Costa, M., Raich, W., Agbunag, C., Leung, B., Hardin, J., & Priess, J. R. (1998b). A Putative Catenin-Cadherin System Mediates Morphogenesis of the Caenorhabditis elegans Embryo. In *The Journal of Cell Biology* (Vol. 141, Issue 1). http://www.jcb.org*develop_120_4_827*. (n.d.).

Ettensohn, C. A. (1985). Mechanisms of Epithelial Invagination. In *Source: The Quarterly Review of Biology* (Vol. 60, Issue 3).

Keller, R. (2006). Mechanisms of elongation in embryogenesis. In *Development* (Vol. 133, Issue 12, pp. 2291–2302). https://doi.org/10.1242/dev.02406

Klein, G., Langegger, M., Timpl, R., & Ekblom, P. (1988). Role of laminin a chain in the development of epithelial cell polarity. *Cell*, *55*(2), 331–341. https://doi.org/10.1016/0092-8674(88)90056-6

Kolahi, K. S., White, P. F., Shreter, D. M., Classen, A. K., Bilder, D., & Mofrad, M. R. K. (2009). Quantitative analysis of epithelial morphogenesis in Drosophila oogenesis: New insights based on morphometric analysis and mechanical modeling. *Developmental Biology*, *331*(2), 129–139. https://doi.org/10.1016/j.ydbio.2009.04.028

Lamiré, L.-A., Milani, P., Runel, G., Kiss, A., Arias, L., Vergier, B., Das, P., Cluet, D., Boudaoud, A., & Grammont, M. (2018). *Gradient in cytoplasmic pressure in the germline cells controls overlying epithelial cell morphogenesis*. https://doi.org/10.1101/440438

Lechler, T., & Fuchs, E. (2005). Asymmetric cell divisions promote stratification and differentiation of mammalian skin. *Nature*, *437*(7056), 275–280. https://doi.org/10.1038/nature03922

Liesa, M., & Shirihai, O. S. (2013). Mitochondrial dynamics in the regulation of nutrient utilization and energy expenditure. *Cell Metabolism*, 17(4), 491-506

Li, J., Economou, A. D., Vacca, B., & Green, J. B. A. (2020). Epithelial invagination by a vertical telescoping cell movement in mammalian salivary glands and teeth. *Nature Communications*, *11*(1). https://doi.org/10.1038/s41467-020-16247-z

Li, J., Wang, Z., Chu, Q., Jiang, K., Li, J., & Tang, N. (2018). The Strength of Mechanical Forces Determines the Differentiation of Alveolar Epithelial Cells. *Developmental Cell*, *44*(3), 297-312.e5. https://doi.org/10.1016/j.devcel.2018.01.008

Melani, M., Simpson, K. J., Brugge, J. S., & Montell, D. (2008). Regulation of Cell Adhesion and Collective Cell Migration by Hindsight and Its Human Homolog RREB1. *Current Biology*, *18*(7), 532–537. https://doi.org/10.1016/j.cub.2008.03.024

Miller, D. E., Cook, K. R., Hemenway, E. A., Fang, V., Miller, A. L., Hales, K. G., & Hawley, R. S. (2018). The molecular and genetic characterization of second chromosome balancers in Drosophila melanogaster. *G3: Genes, Genomes, Genetics*, *8*(4), 1161–1171. https://doi.org/10.1534/g3.118.200021

Nishimura, T., & Takeichi, M. (2009). Chapter 2 Remodeling of the Adherens Junctions During Morphogenesis. *Current Topics in Developmental Biology*, *89*, 33–54. https://doi.org/10.1016/S0070-2153(09)89002-9

Parker, S. E., Mai, C. T., Canfield, M. A., Rickard, R., Wang, Y., Meyer, R. E., Anderson, P., Mason, C. A., Collins, J. S., Kirby, R. S., & Correa, A. (2010). Updated national birth prevalence estimates for selected birth defects in the United States, 2004-2006. *Birth Defects Research Part A - Clinical and Molecular Teratology*, *88*(12), 1008–1016. https://doi.org/10.1002/bdra.20735

Pece, S., & Gutkind, J. S. (2000). Signaling from E-cadharins to the MAPK pathway by the recruitment and activation of epidermal growth factor receptors upon cell-cell contact formation. *Journal of Biological Chemistry*, *275*(52), 41227–41233. https://doi.org/10.1074/jbc.M006578200

Pinheiro, D., & Bellaïche, Y. (2018). Mechanical Force-Driven Adherens Junction Remodeling and Epithelial Dynamics. In *Developmental Cell* (Vol. 47, Issue 1, pp. 3–19). Cell Press. https://doi.org/10.1016/j.devcel.2018.09.014

Priess, J. R., & Hirsh, D. I. (1986). Caenorhabditis elegans morphogenesis: The role of the cytoskeleton in elongation of the embryo. *Developmental Biology*, *117*(1), 156–173. https://doi.org/10.1016/0012-1606(86)90358-1

Rasmussen, J. P., Reddy, S. S., & Priess, J. R. (2012). Laminin is required to orient epithelial polarity in the C. elegans pharynx. *Development*, *139*(11), 2050–2060. https://doi.org/10.1242/dev.078360

Riveline, D., Zamir, E., Balaban, N. Q., Schwarz, U. S., Ishizaki, T., Narumiya, S., Kam, Z., Geiger, B., & Bershadsky, A. D. (2001). Focal Contacts as Mechanosensors: Externally Applied Local Mechanical Force Induces Growth of Focal Contacts by an mDia1-dependent and ROCK-independent Mechanism ✪. In *The Journal of Cell Biology* (Vol. 153, Issue 6). http://www.jcb.org/cgi/content/full/153/6/1175

Sellers, J. R., Chantler, P. D., & Szent-Györgyi, A. G. (1980). Hybrid formation between scallop myofibrils and foreign regulatory light-chains. *Journal of Molecular Biology*, *144*(3), 223–245. https://doi.org/10.1016/0022-2836(80)90088-1

Shindo, A. (2018). Models of convergent extension during morphogenesis. In *Wiley Interdisciplinary Reviews: Developmental Biology* (Vol. 7, Issue 1). John Wiley and Sons Inc. https://doi.org/10.1002/wdev.293

Stewart, M. P., Helenius, J., Toyoda, Y., Ramanathan, S. P., Muller, D. J., & Hyman, A. A. (2011). Hydrostatic pressure and the actomyosin cortex drive mitotic cell rounding. *Nature*, *469*(7329), 226–231. https://doi.org/10.1038/nature09642

Sutherland, A., Keller, R., & Lesko, A. (2020). Convergent extension in mammalian morphogenesis. In *Seminars in Cell and Developmental Biology* (Vol. 100, pp. 199–211). Elsevier Ltd. https://doi.org/10.1016/j.semcdb.2019.11.002

Tepass, U., Theres, C., & Knust, E. (1990). crumbs encodes an EGF-like protein expressed on apical membranes of Drosophila epithelial cells and required for organization of epithelia. *Cell*, *61*(5), 787–799. https://doi.org/10.1016/0092-8674(90)90189-L

Tomer, D., Chippalkatti, R., Mitra, K., & Rikhy, R. (2018). ERK regulates mitochondrial membrane potential in fission deficient Drosophila follicle cells during differentiation. *Developmental Biology*, *434*(1), 48–62. https://doi.org/10.1016/j.ydbio.2017.11.009

Wang, Q., & Margolis, B. (2007). Apical junctional complexes and cell polarity. In *Kidney International* (Vol. 72, Issue 12, pp. 1448–1458). Nature Publishing Group. https://doi.org/10.1038/sj.ki.5002579

Whitehead, J., Vignjevic, D., Fütterer, C., Beaurepaire, E., Robine, S., & Farge, E. (2008). Mechanical factors activate β-catenin-dependent oncogene expression in APC 1638N/+ mouse colon. *HFSP Journal*, *2*(5), 286–294. https://doi.org/10.2976/1.2955566

Wodan, A., Hinz, U., Engelbert, M., & Knust, E. (1995). Expression of Crumbs Confers Apical Character on Plasma Membrane Domains of Ectodermal Epithelia of Drosophila. In *Cell* (Vol. 62).

Yang, Z., Zhao, X., Xu, J., Shang, W., Tong, C., & Liu, Y. (2014). Mitochondrial fission protein Drp1 regulates mitochondrial morphology and cell proliferation by controlling cyclin E signaling. *Oncogene*, 33(5), 519-530.

Google images